C. T. Jolink

Magnetic Stray Field Analysis to Detect Plastic Deformation in Steel Cylinders

Experimental Research into Magnetomechanical Effect Under Impact Loading

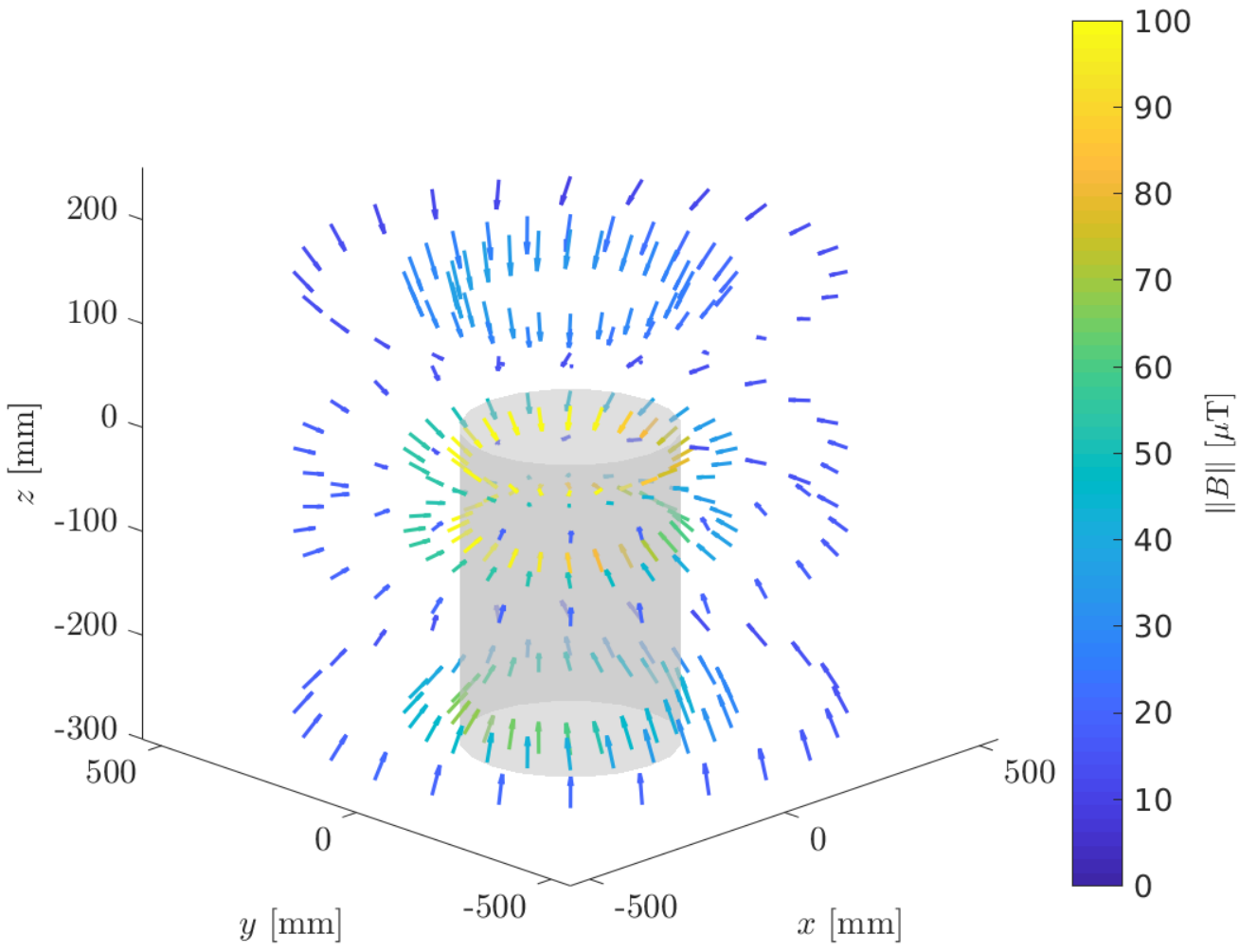

TU Delft

Magnetic Stray Field Analysis to Detect Plastic Deformation in Steel Cylinders

Experimental Research into Magnetomechanical Effect Under Impact Loading

By

C. T. Jolink

in partial fulfilment of the requirements for the degree of

Master of Science
in Civil Engineering

at the Delft University of Technology,
to be defended publicly on Wednesday December 12, 2018 at 5:00 PM.

Supervisor:	Prof. dr. ir. A.V. Metrikine,	TU Delft
Thesis committee:	Dr. ir. A. Tsouvalas,	TU Delft
	Ir. P.C. Meijers,	TU Delft

TU Delft

“We keep moving forward, opening new doors, and doing new things, because we're curious and curiosity keeps leading us down new paths.”

- Walt Disney

Preface

This report finalises my study on ‘Magnetic stray field analysis to detect plastic deformation in steel cylinders’ as my master thesis, in partial fulfilment of my M.Sc.-graduation at the faculty of Civil Engineering and Geosciences of Delft University of Technology. This study focuses on the experimental research into the magnetomechanical effect under impact loading for structural scale cylinders, that I carried out as my graduation project.

My interest in physics was sparked at an early age. I remember it vividly, when my mother bought me books for children, explaining interesting physical phenomena. I read those books front to back in fascination. In elementary school, I wrote an essay about magnetism out of curiosity where these strange, invisible forces were coming from. Little did I know, where this curiosity would lead me. It comes at no surprise that physics was my favourite subject in high school. It was the same curiosity that led me to do a minor in Applied Physics during my bachelor years in university, where I would finally learn about the strange, invisible forces in a course on electrodynamics and magnetism. At the time, I did not see a practical use for this knowledge as a civil engineer, but the satisfaction of one’s curiosity truly is one of the greatest sources of happiness in life. And now, here I am again: learning and writing about the beautiful phenomenon of magnetism in a civil engineering context.

As engineers, we study and built the world. The real, physical world. Yet many of the courses I studied at Delft University of Technology are very theoretical, where nature is captured in seemingly perfect models that make problems often look simpler than they really are. During this study, I learned that the real world is not always as perfect as models would lead you to believe. This is very important to realise when trying to interpret data from research or when designing new technology.

I find that in many discussions, on many topics, data is often cited and treated as if the numbers are casted in stone. When you do experimental research yourself, you learn to always question how data was produced; under which assumptions, limitations and inaccuracies. These are very valuable lessons.

I want to thank Prof. dr. ir. Andrei Metrikine for teaching and inspiring me in his excellent course on *Structural Dynamics* and for allowing me to graduate on such a fascinating topic. I want to thank Dr. ir. Apostolos Tsouvalas for his valuable input and for taking seat in my thesis committee.

My gratitude goes out to the support staff at Stevin II and DEMO for their assistance: Peter de Vries, Kees van Beek, Ruben Kunz, Fred Schilperoort, Giorgos Stamoulis, John Hermsen, Leon Roessen, Martin van der Meer, Ton Blom and Maiko van Leeuwen: thank you!

Most of all, I want thank Ir. Peter Meijers, who fought alongside me in the trenches of the Macrolab as a colleague and with whom I shared many conversations and laughs as a friend.

Lastly, I want to express my gratitude to my parents, who I am greatly indebted to for their unconditional support and trust. I truly believe that the books they bought me many years ago and their encouragement of curiosity, have led me here today.

C. T. Jolink
Delft, December 2018

Contents

Abstract

Pile driving can cause plastic deformation to the head of the driven pile, which in turn can lead to connectivity issues when the superstructure is installed. Moreover, plastic deformation reduces the estimated service life of the structure. Therefore, it is necessary to monitor the strain levels during the installation in order to detect if the yield limit is exceeded. Conventional methods to detect this, like strain gauges, can be hard to install and are prone to damage; hence, a non-contact method is favoured. This research focusses on the magnetomechanical effect to detect the onset of plastic deformation in the structure.

The magnetisation process is hysteretic and, thus, inherently irreversible in nature. Therefore, it is difficult to assess if a change in magnetisation is caused by an applied mechanical stress, by a loss of magnetic properties due to plastic deformation, or by the hysteresis. Previous research suggests, however, that a magnetic equilibrium state can be reached by mechanically stressing the object. When such a magnetic equilibrium is reached, differentiating between the causes of the irreversible changes becomes possible.

In this work, a steel cylinder, 1500 mm tall and 400 mm in diameter, was subjected to repeated axial impact loading in the Stevin II Macro Laboratory of Delft University of Technology. It was observed that the magnetisation of the cylinder reaches an equilibrium state that depends on the initial magnetic state and the maximum induced mechanical stress. Once a magnetic equilibrium state is reached, reversible changes are still observed during impact independent of the maximum induced mechanical stress; irreversible changes, however, only occur when the previous maximum stress is exceeded. Upon increasing the maximum stress, a new equilibrium position is reached. These equilibria follow a trend towards the anhysteretic magnetic state. The equilibrium states that are reached from different initial states do not necessarily coincide.

As soon as plastic deformation at the pile head occurs, an irreversible change in the magnetic stray field is observed. The irreversible change deviates from the trend towards the anhysteretic magnetic state, which makes it possible to differentiate the change caused by plasticity from changes due to hysteresis. This change was particularly visible in the direction of the vector field.

In conclusion, it is possible to reach magnetic equilibrium states with impact loading. There are, however, many equilibrium states; not a single (anhysteretic) equilibrium state can be reached. Nevertheless, it was possible to detect plastic deformation from the magnetic stray field due to a trend deviation. Magnetic stray field analysis may therefore be a viable method to detect plastic deformation in a non-contact manner.

Additionally, a direct correlation was found between the mechanical stress pulse and the magnetic stray field during impact. Although some filtering of the signal is required due to rigid body motions, it seems feasible to monitor dynamic stress pulses at a high sampling frequency through the magnetic field as well, on the condition that irreversible changes in the magnetisation have subsided.

1 Introduction

1.1. General

Many superstructures rely on large columns embedded in the soil as a foundation. One example of such a structure is an (offshore) wind turbine, where steel monopiles are commonly used as a support structure. A monopile is a thin-walled cylindrical structure, consisting of several circular steel tubes that are welded together to form one piece. The largest monopiles to date are over 84 m long, with a diameter of 7.8 m. Monopiles of such dimensions typically reach tens of meters into the soil, so the installation requires an enormous amount of input energy.

To install the pile, a hydraulic impact hammer is positioned at the head of the pile. The hydraulic impact hammer delivers a series of blows to the head of the pile, which then gradually drives the pile into the soil. Depending on the soil conditions, pile dimensions and input energy of the hydraulic hammer, it requires hundreds or even thousands of blows to install the pile (Tsouvalas, 2015). Each blow of the hammer results in very high stresses in the material, particularly at the head of the pile where stress concentrations occur. When the stress in the pile exceeds the yield limit of the material, it will result in plastic deformation.

Traditionally, grouted connections were used between the support structure and the superstructure. Nowadays, bolted connections or slip-joint connections are favoured. For these types of connections, permanent deformations to the pile head can lead to significant connectivity issues, which, in turn, lead to delays and high costs during the installation. Furthermore, material damage in the pile has a detrimental effect on the service life of the support structure, which increases the total cost even further.

One of the paramount challenges of offshore wind energy is to reduce cost, in order to make it a viable option on the growing market for renewable energy. Monitoring the structural health of the monopile in real time during installation is therefore essential to avoid plastic deformation caused by the pile driving process. Conventional methods to measure deformations are contact based, which means that strain gauges are attached with an adhesive to the head of the pile. Installing these strain gauges is a difficult and precise task, which is often cumbersome under harsh conditions. Furthermore, such contact based devices can easily break due to the rough nature of pile driving. A non-collocated technique, i.e. based on measurements on a different location than the plastic zone, to detect plastic deformation is therefore favourable (Meijers, Tsouvalas, and Metrikine, 2018).

This study explores a promising alternative based on the ferromagnetic properties of steel and the magnetomechanical effect. Due to the magnetomechanical effect, changes in the magnetic properties of the material can be observed as a consequence of mechanical stress and plastic deformation. This opens up the possibility to monitor deformations by analysing the magnetic stray field that surrounds the pile.

The phenomenon of magnetism is well understood and the theory is very well developed on an elementary level. However, the theory of magnetic behaviour of ferromagnetic materials and its interaction with mechanical stress is much less developed. The magnetomechanical effect has mainly been studied on relatively small objects in well controlled environments and for quasi-static mechanical loading. Very little is known on a structural scale, especially when the structure is undergoing dynamic loading. For practical applications of the magnetomechanical effect on large scale structures, further investigation in uncontrolled environments is necessary.

In this study we investigate a steel cylinder, 1500 mm tall and 400 mm in diameter that is axially loaded by a drop weight, which resembles the piling process of a monopile and a hydraulic impact hammer on an approximate 1:20 scale. The challenge we face is to distinguish changes in the magnetic stray field around the pile as a consequence of applied stress, of the introduction of plasticity or of other magnetic properties. Section 1.2 introduces some general magnetic phenomena that are relevant to this case and in section 1.3 the precise aim and scope of the research is elaborated.

1.2. Magnetic phenomena

First, we take a look at the physics of magnetic phenomena. Magnetism is most commonly known from magnets: objects that attract magnetic materials such as iron and attract or repel other magnets. To understand how objects become magnetic, we first need to understand what magnetism really *is* and where it comes from on a microscopic level. We first discuss the general relationship between electric and magnetic phenomena and how *magnetic fields* are formed.

We then address how materials can produce a magnetic field and why some materials are affected differently by these fields than others. We also look at macroscopic phenomena of magnetism in materials. This includes how magnetic activity of the material in the past is "memorised" and affects the magnetic behaviour of the material in the future, as well as the interaction between this "magnetic memory" and mechanical activity.

1.2.1. General

Until the beginning of the 19th century, electricity and magnetism were entirely separate subjects. One dealt with the attraction and repulsion of electrical charges and currents while the other dealt with bar magnets and compasses. It was in 1820 that Oersted noticed that an electric current could deflect a magnetic compass needle. Ampère postulated shortly after that all magnetic phenomena are due to moving electric charges. In 1831, Faraday discovered that a moving magnet generates an electric current. Since the development of Maxwell's equations in 1865, electricity and magnetism are unquestionably recognised as two parts of the same phenomenon: **electromagnetism**.

The fundamental problem that the theory of electromagnetism hopes to solve is what influence an electric charge has on another electric charge at a distance. The classical solution takes the form of a field theory: we say that the space around an electric charge (we call this the *source charge*) is permeated by electric and magnetic **fields**. When another electric charge (we call this the *test charge*) is in the presence of these fields, it experiences a force. The field transmits the influence from one charge to the other.

Consider the special case of a wire with a steady current running through it. A steady current means that a stream of (negatively charged) electrons flows through the wire at a steady pace. In the wire, there is an equal amount of stationary positive charges as moving negative charges on any given segment, so the wire is electrically neutral. A *stationary* test charge near the wire would experience no force acting on it. A *moving* charge, however, would be attracted to or repelled from the wire, depending on the direction it is moving relative to the current. The force that accounts for the attraction or repulsion of moving charges is a *magnetic* force. Whereas a *stationary* range produces only an electric field $\mathbf{E}$ in the space around it, a

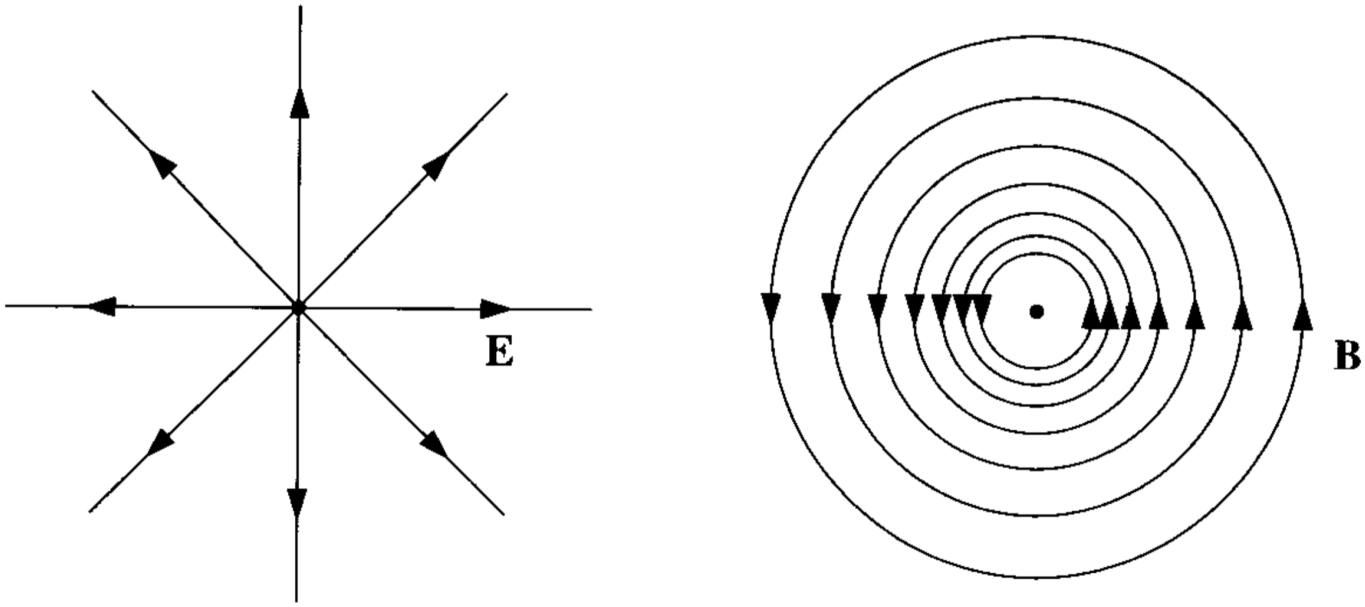

FIGURE 1.1: ELECTROSTATIC FIELD OF A POINT CHARGE (LEFT) AND A MAGNETO STATIC FIELD OF A LONG WIRE (RIGHT) (GRIFFITHS. 2008).

moving charge also generates a magnetic field $\mathbf{B}$. Steady currents produce magnetic fields that are constant in time; the theory of steady currents is called **magnetostatics**.

Magnetic fields can easily be detected using a compass: the needle points in the direction of the local magnetic field. This direction is ordinarily called *north*, in response to Earth's magnetic field that points towards the north. When holding a compass near a current carrying wire, one would find that the needle does not point towards the wire or away from it, but that it circles around the wire.

Electric fields originate on positive charges and terminate on negative ones; magnetic field lines do not begin or end anywhere, as that would require a non-zero divergence. They always form closed loops or extend out to infinity. This is a fundamental difference with electrostatics, because there are no point sources for $\mathbf{B}$, as there are for $\mathbf{E}$; there exists no magnetic analog to electric charge. It was long believed that magnetism was produced by magnetic charges (or **magnetic monopoles**), but as far as we know now, these do not exist. Therefore, magnetostatic fields look quite different from electrostatic fields (figure 1.1).

While we cannot create a field similar to the electric monopole, we can devise a current distribution whose magnetic field resembles the electric dipole (figure 1.2). A **magnetic dipole** can be created with a very small **current loop**. For a true dipole, the current loop would have to be infinitesimally small, but in practice, a dipole is a suitable approximation whenever the distance r greatly exceeds the size of the loop. Such small currents can easily be found in nature, like spinning electrons or electrons orbiting a nucleus.

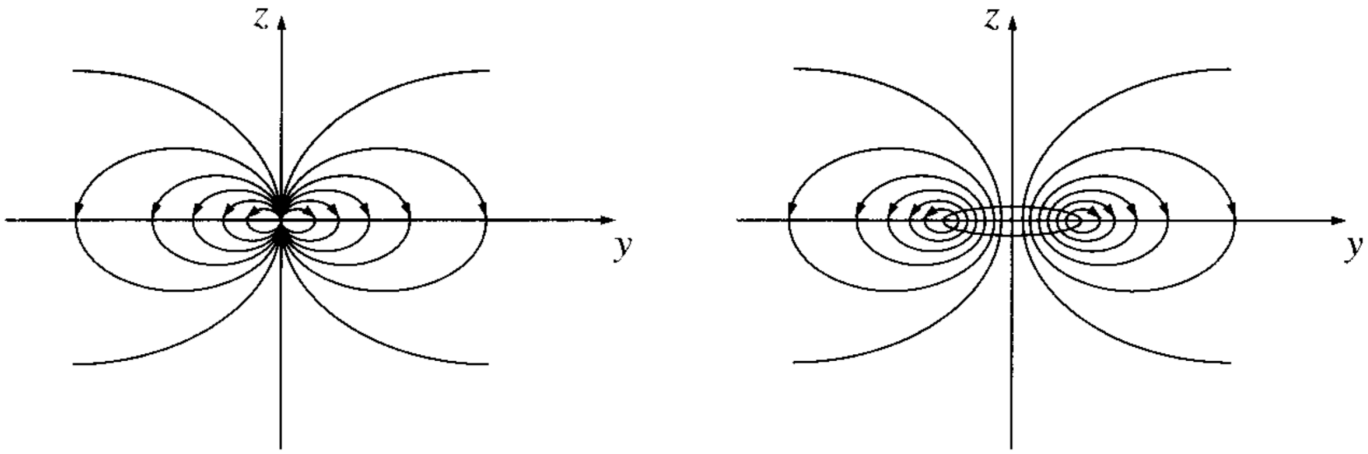

FIGURE 1.2: FIELD OF A "PURE" DIPOLE (LEFT) AND OF A "PHYSICAL" DIPOLE (RIGHT) (GRIFFITHS, 2008).

1.2.2. Materials

The most common understanding of magnetism is related to magnetic materials, which has no obvious connection with moving charges or current-carrying wires. Yet all magnetic phenomena are due to electric charges in motion. It is due to the spinning and orbiting of electrons in materials - which can be considered as tiny currents - that we find a magnetic field around certain materials. For macroscopic purposes, these currents are so small that we can treat them as dipoles. In fact, *all* materials have these dipoles, but due to their random orientation, their effects cancel out. These dipoles are intrinsic characteristics of elementary particles and are called the **intrinsic magnetic moment** m. These dipoles can be imagined as tiny bar magnets on an atomic scale. When a net alignment of these magnetic dipoles occurs, the medium becomes magnetically polarised, or **magnetised**. By integrating the contribution of magnetic moments over the volume of the material, one can define the macroscopic magnetisation $\mathbf{M}$:

$$\mathbf{M} = \int m\, dV \tag{1.1}$$

Alignment of magnetic dipoles occurs due the the influence of an external magnetic field. In the presence of an external magnetic field $\mathbf{B}$, dipoles in a material may align parallel to $\mathbf{B}$ (called **paramagnets**) or

antiparallel to $\mathbf{B}$ (called **diamagnets**). When the external magnetic field is removed, the dipoles in paramagnets and diamagnets will lose their alignment and return into a random orientation. A third category of materials is called a **ferromagnet** (named after the most common example, iron), more commonly known as **permanent magnets**. Ferromagnets retain their magnetisation even after the external field has been removed. For these materials, the magnetisation is not determined by the present field but by the whole magnetic "history" of the object.

Unlike paramagnets, ferromagnets are emphatically non-linear. What makes ferromagnets different from paramagnets is the interactions between nearby dipoles: in a ferromagnet, dipoles 'like' to point in the same direction as their neighbours. In a very strong permanent magnet, nearly all these dipoles point in the same direction and reinforce each other. The reason that everyday metal object do not typically behave as permanent magnets, is that the alignments of dipoles occur in small volumes, called **domains**. Each domain contains billions of dipoles that are aligned within the domain, but the domains themselves can be oriented at different angles. Metal objects contain an enormous amount of domains, so their magnetic fields tend to cancel.

When an external field is applied to the material, the dipoles will experience a torque, forcing them to align with the external field. The interaction with their neighbours is typically strong enough to resist this torque. However, at the boundary between two domains, there are 'competing' neighbours and the torque will reinforce the influence of the domain most parallel to the field. Dipoles at the boundaries of a domain will therefore align with this domain at the expense of the less favourable oriented domain (figure 1.3). As a result, one domain expands while the other domain becomes smaller. The boundary, also called a **domain wall**, will move. If the field is strong enough, one domain can take over entirely and the material is considered "saturated".

The process of moving domain walls is partially, but not entirely irreversible. Hence when the external field is removed, there remains a predominance of domains and the object can be considered magnetised. This effect is called **hysteresis**.

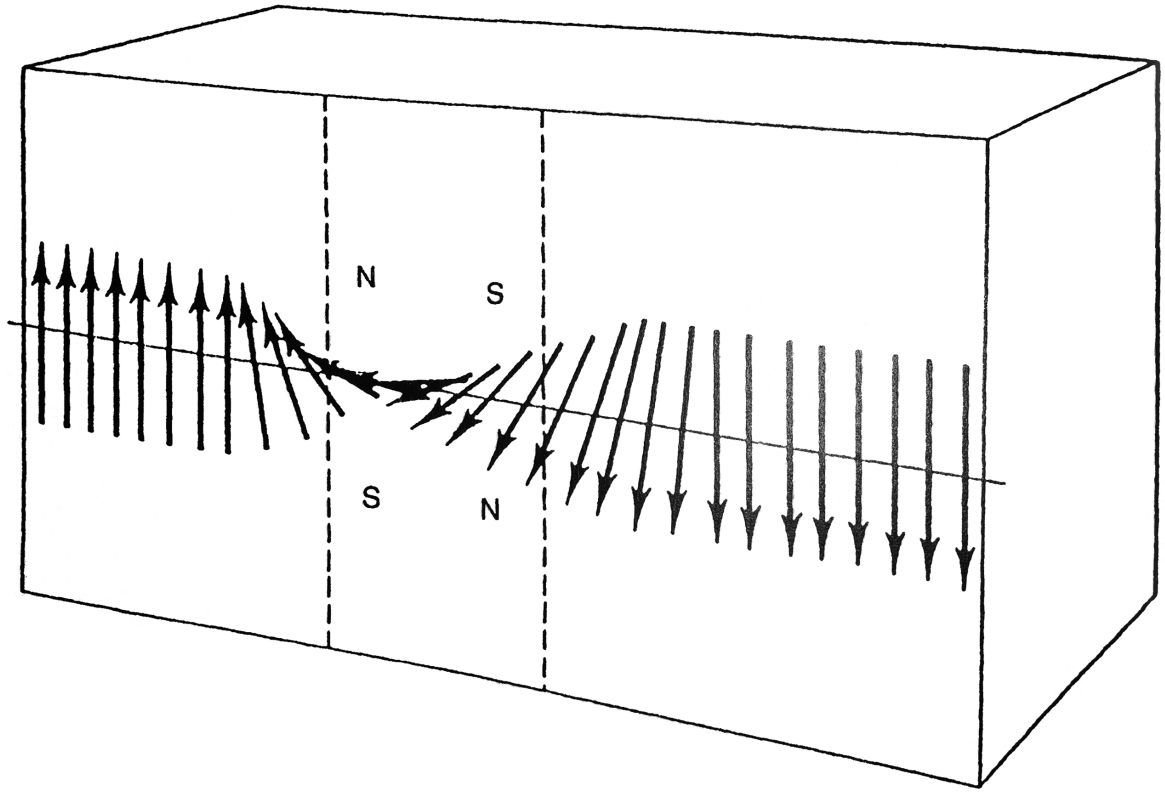

FIGURE 1.3: ALIGNMENT OF MAGNETIC DIPOLES IN A 180º DOMAIN WALL (JILES, 1998).

The translation of domain walls can be impeded by local impurities in the material. Isolated regions with magnetic properties different from the main magnetic material are known as magnetic inclusions; these may be oxides or carbides, pores, voids, cracks or other mechanical inhomogeneities. When a domain wall intersects one of these inclusions, the energy of the domain wall is reduced. Consequently, the domain walls are attracted to the inclusion which then effectively impedes the wall motion. These impurities are then called **pinning sites**, which provide local energy barriers which the domain walls need to overcome (Jiles, 1998).

While applying an external magnetic field to a ferromagnetic material causes domain walls to move, a similar event can be observed when mechanical stress is applied to the material. The magnetisation of an object and the mechanical stress that is applied to it, are inherently linked. This is called the **magnetomechanical effect**. The stress in the material can therefore be modelled as a locally applied, effective magnetic field (Jiles, 1998). For this reason, local residual strains in the material due to plastic deformation act as magnetic inclusions. Hence, the more plastic deformation occurs, the harder it becomes for domain walls to move and for the object to become magnetised. An irreversible change in the magnetic stray field of the object should therefore happen when plastic deformation is induced.

The hysteretic nature of magnetisation makes it difficult to assess what causes the (irreversible) change. After all, each stress cycle acts as an applied external magnetic field, which can move the domain walls and alter the effective stray field. It is therefore far from trivial to assess if the magnetic signature changes because the domain walls move towards an energetically more favourable state, or if additional pinning sites due to plastification alter the most favourable state.

1.3. Aim and scope

This study aims at providing an answer to the usability of magnetic stray field analysis to detect plastic deformation caused by pile driving. To make this method usable in practice, it should be researched on a structural scale and in uncontrolled conditions: Earth's field should not be cancelled and other variables like temperature should be similar to real life conditions. Measuring the magnetic field should be non-contact based, preferable away from the area where plastic deformation is prone to occur.

The main challenge we face is how to distinguish changes in the magnetic stray field caused by plastification from changes due to active loading and the hysteretic nature of ferromagnetism. The fundamental idea to do so is that a magnetic equilibrium state exists where all domains are oriented such that the energy of domain walls is minimised. This is called the **anhysteretic state**, from where all mechanically induced changes are reversible. If such a state can be reached within the elastic regime, then all irreversible changes thereafter can be contributed to permanent changes in the structure, i.e. plastic deformation. The general idea is that the magnetisation of the structure, independently of its initial state, will always move towards this anhysteretic state when mechanically stressed. Previous research by Jiles and Atherton (1984) , Pitman (1990), Jiles (1995), Viana et al. (2010) and Li et al. (2017) support this idea, although most research focusses on small scale objects, loaded quasi-statically in tension. If the anhysteretic state can be reached by loading a structural scale object with dynamic impact loading, independent of its initial magnetic state, remains to be seen.

This is what this study focusses on with the following research questions:

- "Will the magnetisation of a steel cylinder with unknown initial magnetisation reach a specific and consistent equilibrium state from repeated impact loading within the elastic regime?"

- "If an equilibrium state can be reached, can we distinct irreversible changes in magnetisation from different causes to detect plasticity?"

The research of this thesis is oriented on experimental observations, in order to test the predictions that were deducted from the hypothesis that the magnetisation of an object will always progress to an equilibrium state after being loaded with repeated impacts. A few considerations are to be made for the experiment:

1. While it would be useful to be able to control the external magnetic field in order to assess its influence, this is not possible without an advanced field-canceling set-up, like a Helmholtz coil. Given the scale of the experiment, this is not feasible and we have to compromise to an uncontrolled background field.

2. A few assumptions need to be made, including:

    1. The stress distribution in the cylinder is considered to be uniform. In reality, this is certainly not the case, because the cylinder will always be hit somewhat asymmetrically. Therefore, stress concentrations occur, especially near the head of the pile. The stress will be distributed more evenly at a distance from the head;

    2. The drop weight is considered to fall freely under gravity, with little or no friction. Each impact from the same height is considered the same, although variations in induced stress are observed;

    3. Earth's magnetic field is considered constant in time.

3. The experiment is limited in a few ways:

    1. The size of the cylinder and the total set-up is chosen to be as large as possible within practical limitations and commercial availability. This limitation affects the length, diameter and wall thickness of the cylinder and the true to scale resemblance of a structural monopile;

    2. Drop weights are limited to approximately 600 kg and the maximum drop height is limited to 5 m.

    3. To avoid interference in the magnetic measurements, all components of the set-up near the locations of the magnetic sensors need to be non-magnetic. This limits the construction to materials such as concrete, timber, aluminium and stainless steel;

    4. Measuring the magnetic field at many locations during and after each impact, is very time consuming or would significantly drive up the cost. Measurement locations are, therefore, limited to 12 rings near the head of the pile for static measurements and 1 fixed location for dynamic measurements;

    5. The high forces and the rough nature of this experiment limit the accuracy of measurements, because the distance of the sensor to the pile may vary slightly in between blows due to rigid body motions of the pile;

    6. While the boundary conditions of the cylinder are carefully considered, there are practical limitations in preventing rigid body motion and reflections of stress waves.

4. Some generalisations are made:

    1. The cylinder in the experiment can be considered to be very short compared to a monopile and traveling waves in a monopile will look quite different compared to the strain signal observed in this experiment. However, the observed magnetic events are considered as a good representation of what would happen in a longer pile;

    2. The stress signal that is induced by a concrete drop weight will be quite different from that of a hydraulic impact hammer, mainly because the drop weight is relatively long compared to the pile and the time-strain signal will therefore be much longer than usual. This signal is nevertheless considered as a good representation of that of a hydraulic impact hammer.

1.4. Outline

In chapter 1 we have so far analysed a problem and defined the goal of this thesis. We have set the scope and methodology of the experimental research, where compromises, generalisations, assumptions and limitations are discussed.

Chapter 2 is devoted to the scientific paper. The paper starts with a brief introduction to the problem, like section 1.1. Literature study discusses previous observations on the magnetomechanical effect, why these observations lead to before mentioned hypothesis and why it is necessary to experiment on a large scale object under impact loading.

The paper then discusses the theory and the empirical model behind the magnetomechanical effect, as it was introduced by Jiles (1995). The experimental setup is discussed in detail, as well as the procedure of tests that were conducted. Results of the tests are shown, where it becomes clear what the shape of the magnetic stray field looks like and how it is altered as a result of the impact loading. Changes in both the elastic and plastic regime are observed. A discussion about these results follows, reflecting on the theory and practical usability of this technique to detect plastic deformation, according to these results. The paper ends with conclusions.

Note that the paper forms an entity on itself and can be read independently of the rest of this report. Therefore, an overlap in the introduction and conclusion of the paper and this report is to be expected.

During the experiment, a few discoveries came to light that are outside of the scope of the research and are not discussed in the paper, but are still of great value for other purposes. These findings are briefly discussed in chapter 3. These findings include the direct correlation between the dynamic time-strain signal and the magnetic flux signal during impact and on what conditions the magnetic flux signal could be used as an alternative to strain gauges to monitor dynamic stress pulses.

Chapter 4 recaps the conclusions of the experiment and adds recommendations. These recommendations include improvements to the used set-up, future tests and improvements to the model.

Appendix A provides additional images and drawings of the experimental set-up.

2 Paper

Magnetic stray field analysis of a steel circular cylinder subjected to repeated axial impact loading

C.T. Jolink, P.C. Meijers[1], A. Tsouvalas, A.V. Metrikine.

Abstract

Pile driving can cause plastic deformation to the head of the driven pile, which in turn can lead to connectivity issues when the superstructure is installed. Moreover, plastic deformation reduces the estimated service life of the structure. Therefore, it is necessary to monitor the strain levels during the installation in order to detect if the yield limit is exceeded. Conventional methods to detect this, like strain gauges, can be hard to install and are prone to damage; hence, a non-contact method is favoured. This research focusses on the magnetomechanical effect to detect the onset of plastic deformation in the structure.

The magnetisation process is hysteretic and, thus, inherently irreversible in nature. Therefore, it is difficult to assess if a change in magnetisation is caused by an applied mechanical stress, by a loss of magnetic properties due to plastic deformation, or by the hysteresis. Previous research suggests, however, that a magnetic equilibrium state can be reached by mechanically stressing the object. When such a magnetic equilibrium is reached, differentiating between the causes of the irreversible changes becomes possible.

In this work, a steel cylinder, 1500 mm tall and 400 mm in diameter, was subjected to repeated axial impact loading in the Stevin II Macro Laboratory of Delft University of Technology. It was observed that the magnetisation of the cylinder reaches an equilibrium state that depends on the initial magnetic state and the maximum induced mechanical stress. Once a magnetic equilibrium state is reached, reversible changes are still observed during impact independent of the maximum induced mechanical stress; irreversible changes, however, only occur when the previous maximum stress is exceeded. Upon increasing the maximum stress, a new equilibrium position is reached. These equilibria follow a trend towards the anhysteretic magnetic state. The equilibrium states that are reached from different initial states do not necessarily coincide.

As soon as plastic deformation at the pile head occurs, an irreversible change in the magnetic stray field is observed. The irreversible change deviates from the trend towards the anhysteretic magnetic state, which makes it possible to differentiate the change caused by plasticity from changes due to hysteresis. This change was particularly visible in the direction of the vector field.

In conclusion, it is possible to reach magnetic equilibrium states with impact loading. There are, however, many equilibrium states; not a single (anhysteretic) equilibrium state can be reached. Nevertheless, it was possible to detect plastic deformation from the magnetic stray field due to a trend deviation. Magnetic stray field analysis may therefore be a viable method to detect plastic deformation in a non-contact manner.

[1] p.c.meijers@tudelft.nl

1. Introduction

Steel monopiles are commonly used foundations for offshore wind turbines; they are thin-walled cylindrical structures which are usually driven into the seabed with hydraulic impact hammers. Each hammer blow at the pile head induces stress waves in the pile, which help the pile to gradually progress into the seabed. During this installation process, plastic deformation may occur at the pile head due to the high impact-induced stresses; this can lead to alignment problems when the offshore wind tower is bolted on top of the pile and to a shortened service life of the structure due to fatigue. To check whether plastic deformation occurs in the pile, it is important to assess the structural health of the monopole in real-time by monitoring the stress levels in the material in a non-destructive manner. Currently, the stress signal generated by the impact hammer can be measured directly by means of strain gauges attached near the pile head. This technique, however, has several drawbacks. First, due to high strain levels generated in this critical area, sensors that are directly attached to the monopile can easily break. Second, such sensors need careful installation, which is difficult given the hard conditions at sea.

To avoid all aforementioned problems, a non-collocated technique to detect and quantify plastic deformation, i.e. based on measurements on a different location than the plastic zone, is therefore favourable. One such methods was recently put forward by Meijers, Tsouvalas, and Metrikine (2018), and it is based on more classical sensors, i.e. strain gauges. It was shown that the amount of plastic deformation caused by a hammer impact is related to the energy loss of the travelling wave which can be measured a distance below the pile head. While avoiding this critical area, this method, however, still requires that the sensors are attached directly to the structure.

A promising alternative based on the magnetic stray field surrounding the monopile is therefore explored in this paper, as the strength and direction of this field depend on the applied mechanical stress and plastic strain levels: the so-called magnetomechanical effect (Bao and Gong, 2012). When ferromagnetic materials like structural steel are stressed in the presence of an external magnetic field, e.g. Earth's magnetic field, they tend to change their magnetisation (Jiles, 1995). Moreover, their ability to magnetise reduces with increasing levels of plastic deformation (Sablik et al., 2010). The magnetic signature of the structure is therefore influenced by deformations in the material in both the elastic and plastic regime.

Complications in the use of this technique to detect plastic deformation in a non-collocated manner arise from the fact that the magnetisation process is hysteretic and, therefore, inherently irreversible in nature (Jiles, 1995). This means that the magnetisation of the material changes upon loading, follows a different path upon unloading and ends up at a different magnetic state when the load vanishes. Thus, it is difficult to assess if a change in magnetisation results from an applied mechanical stress, is caused by a loss of magnetic properties due to plastic deformation or by the non-linear behaviour of the magnetomechanical effect. Fortunately, research by Pitman (1990), Jiles (1995), Viana et al. (2010) and more recently Li et al. (2017), suggest that a magnetic equilibrium state can be reached by mechanically stressing a material. The conclusion of Jiles and Atherton (1984) that all stress induced changes to the magnetisation lead towards the anhysteretic state, is of particular significance.

It is this equilibrium state that could give the possibility to distinguish between a change in magnetisation caused by plastic deformation of the material and a change due to hysteresis, since the latter effect vanishes in the equilibrium state. Hence, the magnetisation of the monopile should be brought in such an equilibrium state to assess whether plastic deformation has occurred.

Early experimental research into the magnetisation changes caused by stress mainly focussed on the effect of a single load-unload cycle, see e.g. Craik and Wood (1970) and Pitman (1990). These experiments were performed on small-scale specimens in a well-controlled laboratory environment. Magnetisation changes of large-scale steel structures have been reported by Atherton (1984) and Viana et al. (2010), indicating that the magnetomechanical effect is also measurable on these scales, although the resulting magnetic field is more complex due to the geometry of the specimens. More recently, the effect of cyclic loading on the magnetisation of steel was investigated by Bao and Gong (2012). Furthermore, Bao et al. (2017) reported that the effect of the loading speed could not be neglected. In all these papers, however, the loading can be considered quasi-static, especially when compared to the time scales associated with dynamical loading induced by an axial impact of the hammer. Therefore, the changes of the magnetic stray field of a large-scale steel structure subjected to repeated axial impacts are investigated in this paper.

The research is oriented around qualitative experimental observations, in order to test the predictions that were deducted from the hypothesis that the magnetisation of an object will always progress to an equilibrium state after being loaded with repeated impacts. Secondly, it is observed if deviations from such equilibria can be linked to plastic deformation on a structural scale. To do so, the piling process with a hydraulic impact hammer is simulated on an approximate 1:20 scale, with a steel cylinder, 1500 mm tall and 400 mm in diameter that is axially loaded by a drop weight.

Similar observations have been reported by aforementioned authors for small scale objects in controlled environments, generally with fundamental scientific purposes in mind. The research in this paper serves a specific practical purpose that has not been reported before: using the trend deviation of magnetic equilibrium states to detect plastic deformation in structural scale piles caused by repeated dynamic impact loading in uncontrolled conditions. It was found that multiple equilibrium states can be reached, but that this has no practical implications for the purpose that is considered.

Section 2 of this paper elaborates on the theory behind the magnetomechanical effect according to the 'Law of Approach' by Jiles (1995). Section 3 describes the experimental set-up and procedure that was used for this research. Section 4 shows the results of the experiment: the changes in magnetisation are compared for different initial states and different mechanical loads. Trends in these changes are evaluated and a deviation of these trends are observed when plastic deformation occurs. Section 5 discusses the possible underlying reasons for these observations. Section 6 finalises this paper with conclusions.

2. Theory

The magnetisation of a steel specimen in a constant weak external magnetic field in the presence of mechanical stress has been investigated both experimentally and theoretically. From these endeavours, the empirical model of Jiles (1995), also referred to as the Law of Approach, has been the most popular so far. The main concept in the model is the experimental observation that the magnetisation of a ferromagnet tends towards the anhysteretic magnetisation curve, which represents a global magnetic equilibrium state.

To simplify the discussion, a one-dimensional approach is considered here; i.e. the external field H_0, the magnetisation M and the stress field σ are all assumed to be aligned along a single axis. As a result, of the vector and tensor expressions for these quantities only a single component remains.

In the Law of Approach, as described in Jiles (1995), the influence of the stress on the magnetisation is captured in the effective field H_e, which depends on the external field, the magnetisation itself and the magnetostriction as follows:

$$H_e = H_0 + \alpha M + \frac{3\sigma}{2\mu_0}\frac{\partial \lambda}{\partial M}. \tag{1}$$

In which α is a coupling constant, μ_0 the permeability of free space and λ the magnetostriction coefficient. The latter is a symmetric function of the magnetisation:

$$\lambda = \left(\gamma_1 + \sigma\gamma_1'\right) M^2 + \left(\gamma_2 + \sigma\gamma_2'\right) M^4, \tag{2}$$

where the γ coefficients are constants. With the effective magnetic field defined, the expression for the anhysteretic magnetisation is

$$\frac{M_{an}}{M_s} = \coth\left(\frac{H_e}{a}\right) - \frac{a}{H_e}, \tag{3}$$

in which a, M_s are model constants. For a given external field strength, this implicit expression for the anhysteretic curve can be solved numerically with the method based on differential equations developed by Viana et al. (2010a). Using the same parameters as those authors, the anhysteretic curve under a constant magnetic field for different uni-axial stress levels is presented in figure 1. It is clear that compressional stresses result in different behaviour than tensile stresses

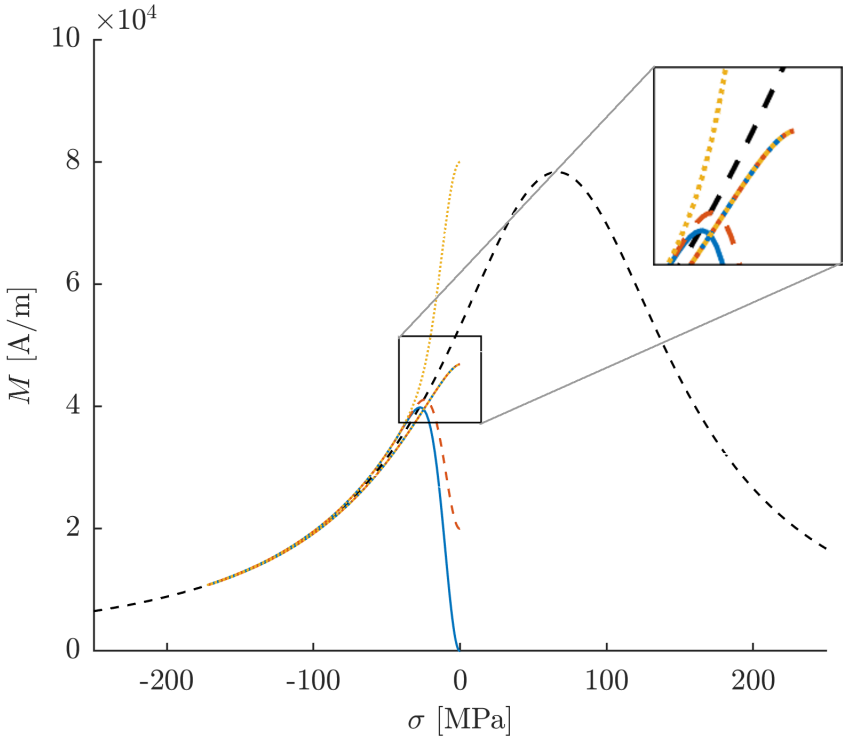

FIGURE 1: ANHYSTERETIC MAGNETISATION FOR H_0 = 26 A/M (DASHED LINE) AND THE LAW OF APPROACH FOR THREE DIFFERENT INITIAL MAGNETISATION LEVELS.

With the anhysteretic curve defined, Jiles derives the change of the magnetisation with changing stress as

$$\frac{\partial M}{\partial \sigma} = \frac{\sigma}{\xi E}\left(M_{an} - M\right) + c\frac{\partial M_{an}}{\partial \sigma}, \tag{4}$$

where ξ and c are model constants, and E the Young's modulus. For a given initial magnetisation, the resulting magnetisation due to a stress signal can be computed. Jiles shows that this works rather well for the available experimental data of Craik and Wood (1970), where a steel specimen is loaded and unloaded once.

Figure 1 shows the results of a simulation of the magnetisation for a single compression loading cycle with three different initial magnetisation levels. All three simulations result in the same remanent magnetisation level, just below the anhysteretic value. When the loading cycle is repeated, the resulting magnetisation at zero stress does not change anymore; this indicates that, if the model is applicable for repeated compressional loading, the resulting stray field does not change after the first cycle and it will reach the same equilibrium value for different stress levels. However, experiments by Maylin and Squire (1993) indicate that the equilibrium value that is reached not necessarily has to be the anhysteretic equilibrium value. To capture this effect, Xu et al. (2012) introduce another equilibrium state which lies around the anhysteretic state: this state they called M_0. This new equilibrium is different as it incorporates the effect of residual pinning sites which are not easily overcome; this is in contrast with the anhysteretic magnetisation where there are no pinning sites.

To incorporate the effect of plastic deformation on the magnetisation, the Law of Approach has been amended later by Sablik et al. (2004). As plastic deformation introduces more dislocations in the material, the number of pinning sites will also increase. This reduces the ability of a material to be magnetised as the pinning sites prohibit the magnetic domains to grow and thus to merge into a larger domain with the same magnetisation. Therefore, when plastic deformation is introduced, the total magnetisation decreases, see e.g. Jiles (1988). This property of ferromagnetic materials should enable one to detect the onset of plastic deformation even on a structural scale.

3. Experimental set-up

The experiment was conducted in Stevin II Macrolab of Delft University of Technology, faculty of Civil Engineering and Geosciences. The experiment resembles the piling process of an offshore monopile on an approximate 1:20 scale.

The specimen is a cold-finished, welded, thin-walled steel cylinder. It is 1500 mm tall, 406 mm in diameter and 8 mm thick. To achieve higher stresses in the material at the impacted end of the cylinder, the top 500 mm was machined to a thickness of 2.5 mm. The steel is S235 with a certified tensile yield stress of 300 MPa. The chemical composition of the material is shown in table 1.

The lower boundary condition of the pile was designed to minimise rigid body motions of the steel cylinder, by bolting the cylinder on a stainless steel plate through a timber core inside the bottom 200 mm of the cylinder, that was then bolted onto timber beams to avoid rigid body motion as a result of plate bending. The stainless steel plate with timber beams is then placed on a 40 mm layer of EVA-foam, while the whole system is weighed down by 300 kg of sand, contained in a timber box. The top boundary of the pile is unsupported

3.1. Dynamic testing

The impact hammer in this experiment is substituted by a drop weight that can fall under the presence of gravity. This weight is a 403.5 kg, cylindrical concrete block. The weight is guided over an aluminium rod, to ensure that the weight is dropped safely and as symmetrically as possible onto the sample.

To avoid interference in the magnetic field measurements, the setup is designed such that no ferromagnetic materials other than the specimen are near the magnetic sensors. The concrete block is therefore not reinforced with steel rebars, but with plastic microfibres instead. A 6 mm circular stainless steel plate is attached to the concrete block on the impact surface. The weight is lifted by a crane and dropped by a mechanical quick-release hook to ensure that the weight can fall freely.

3.2. Sensors and electronics

To measure the static magnetic field in between impacts, a triaxial FLC3-70 fluxgate magnetometer with a resolution of 1 nT is used. Measurements took place at four different heights and at three different radii around the head of the cylinder, as indicated in figure 4. The sensor is rotated 360 degrees around the cylinder, resulting in twelve “rings” of magnetic field measurements. The cumulative error is in the order of 2 μT.

FIGURE 2: THE CYLINDER WITH INSTALLED COIL.

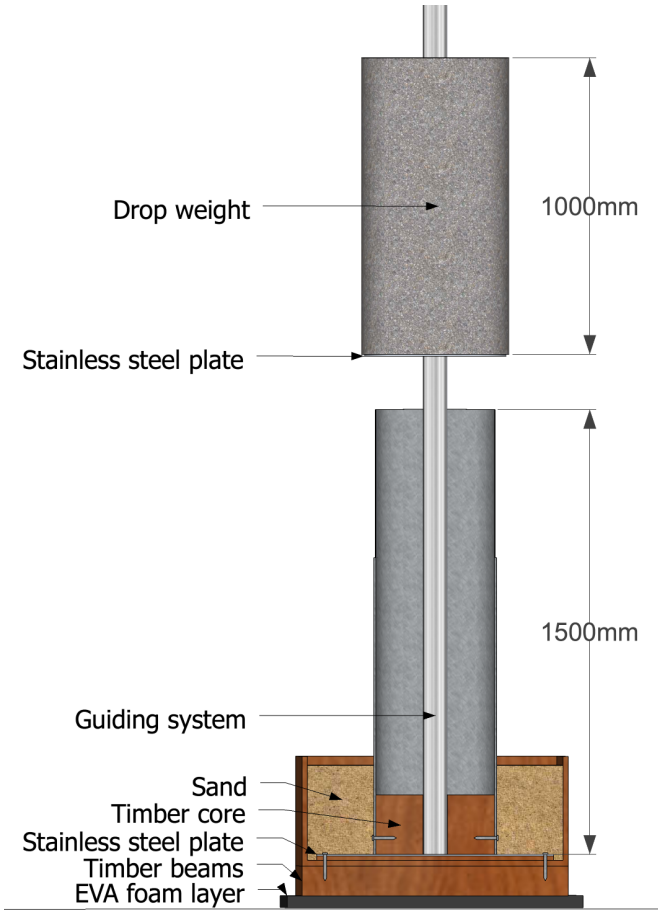

FIGURE 3: SCHEMATIC OF THE SET-UP.

Element	C	Si	Mn	P	S	Cr	Mo	Ni	Al	B	Cu	N	Nb	Sn	Ti	V
%	0.14	0.180	0.79	0.011	0.007	0.017	0.001	0.019	0.040	0.0002	0.016	0.0047	0.001	0.009	0.001	0.002

TABLE 1: CHEMICAL COMPOSITION OF THE STEEL SPECIMEN.

To measure the dynamic magnetic field during impacts, a biaxial HMC1052L AMR sensor with a resolution of 12 nT was used at a 50 kHz sampling rate. Measurements during impact took place at $Z = 200$ mm, $R = 225$ mm, $\theta = 120^{o}$.

Strains in the cylinder are measured with four UFLA-5-11 strain gauges at 50 kHz in a Wheatstone bridge configuration: two on opposite sides at $Z = 200$ mm and two on opposite sides at $Z = 900$ mm.

The cylinder can be magnetised with a coil of 32 windings with a maximum of 10 A, resulting in a field in the cylinder of 80 A/m, located 500 mm from the top of the cylinder. Using this coil, the magnetisation of the cylinder can be brought to a consistent and repeatable state, so multiple tests can be conducted with the same initial conditions. The polarity of the coil can be switched to magnetise the cylinder consistently in opposite direction. Furthermore, a demagnetiser was used to demagnetise the cylinder in between test before magnetising it with the coil. With these tools, the magnetic state of the cylinder can be set to positive and negative remanence on various (minor) hysteresis loops.

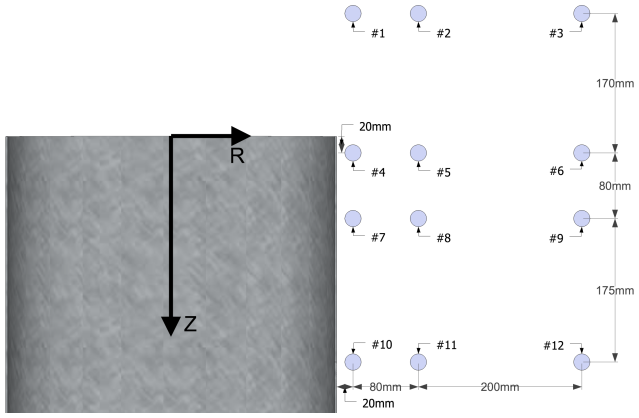

FIGURE 4: MEASURE POINTS NEAR HEAD OF CYLINDER.

3.3. Experiments

The experiments consist of six tests. In all tests, the cylinder is subjected to repeated impacts by dropping the weight axially onto the cylinder until the magnetic field reaches an equilibrium state. The six tests vary in initial magnetic state before inducing mechanical stress and in maximum induced stress level, by varying the drop height.

In this paper, the drop height of the weight is used as a reference for the induced stress. Each drop height corresponds to an average measured peak stress in the thin part of the cylinder, as shown in table 2[2].

Before the cylinder is installed, a background field measurement is recorded on 12 rings near the position of the head of the cylinder, as shown in figure 4. This background field measurement is then subtracted from the measurements with the cylinder installed, in order to find the stray field.

The initial magnetic state and the procedure of impacts for test 1 through 5 are summarised in table 3. For test 2 through 5, the cylinder is magnetised with a strong magnetic field (80 A/m) in either upward or downward direction whereas for test 1, the cylinder is magnetised with a much weaker field so that the initial magnetic state is in between both extremes.

Tests 1, 2 and 3 are performed in two stages. First, the cylinder is loaded with 500 mm impacts until the magnetic field has converged to a certain equilibrium state. The cylinder is then loaded with 1000 mm impacts until a new equilibrium state is reached. For tests 4 and 5, the cylinder is loaded with 1000 mm impacts from the beginning until a magnetic equilibrium state is reached.

Drop height	500 ± 5 mm	1000 ± 5mm	1500 ± 5 mm	2000 ± 5 mm	2500 ± 5 mm
Average peak stress μ (MPa)	119.3	186.2	247.5	317.1	327.8
Standard deviation σ (MPa)	9.22	11.84	20.63	4.96	16.76

TABLE 2: INDUCED STRESS LEVELS DUE TO DIFFERENT DROP HEIGHTS.

[2] Due to residual strains and non-linearity of stress-strain curve, actual stress is lower for 2000 mm and 2500 mm drop height.

Test	Initial magnetisation	First drop height (mm)	Second drop height (mm)
1	Downwards, low field	500	1000
2	Downwards, strong field	500	1000
3	Upwards, strong field	500	1000
4	Upwards, strong field	1000	
5	Downwards, strong field	1000	

TABLE 3: PROCEDURE OF THE EXPERIMENT.

A magnetic equilibrium state is assumed to be reached when for all components of the magnetic field a linear regression line through the last six measurements has changed sign at least once.

For test 6, the cylinder is magnetised “upwards” with a strong field. The cylinder is then repeatedly loaded with drops from increasing height. Starting with 1000 mm, the drop height is increased in 500 mm intervals, every time a new equilibrium state is reached, until plastic deformation occurs.

4. Results

4.1. Dynamic response

Figure 5 shows a typical time-strain signal for a 500 mm drop and a 1000 mm drop. The peak strain is typically reached within 3 ms, which is vastly faster than any quasi-static loading scenario. The total strain signal is less than 30 ms. Each drop consists of three similar peaks in decreasing magnitude, because the drop weight bounces up three times after impact.
Due to the fact that the cylinder is quite short relative to the wave speed, these signals are superimposed standing waves, rather than traveling waves.

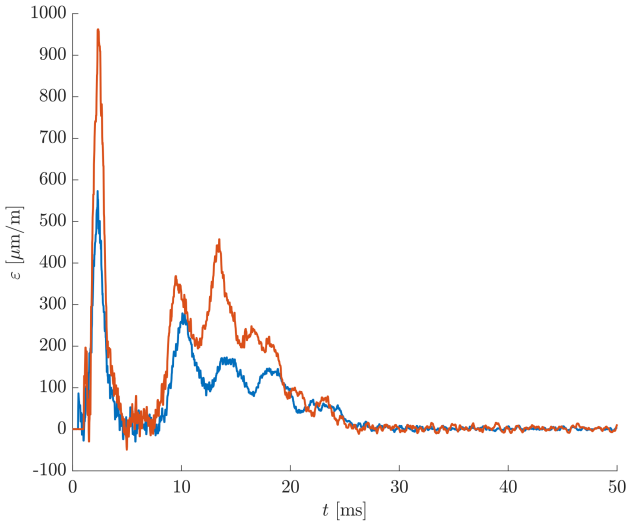

FIGURE 5: A TYPICAL TIME-STRAIN SIGNAL FOR A 500 MM DROP (BLUE) AND A 1000 MM DROP (RED).

4.2. Magnetic background field

Figure 6 shows the direction and magnitude of the background field at the test location. The position of the cylinder is indicated, although the cylinder is not present during the background measurement. As expected from the Earth’s magnetic field, the field is uniform at all measurement rings, indicating that there are no disturbing stray fields in the presence of the set-up. The field has a magnitude of 39.3 μT; the largest component is the downward component measuring 35.3 μT.

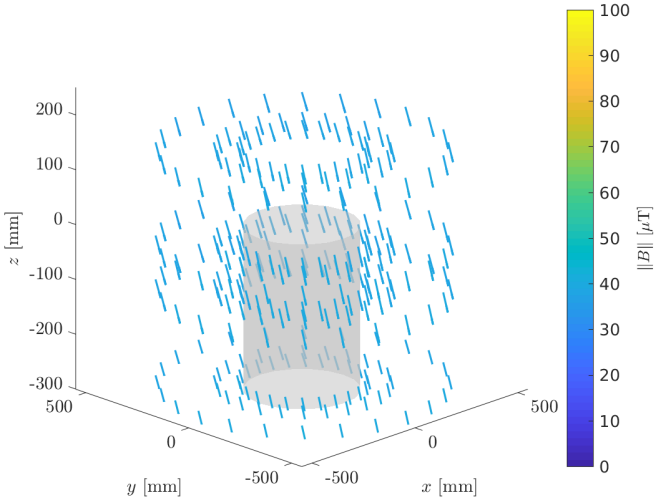

FIGURE 6: BACKGROUND FIELD AT TEST LOCATION.

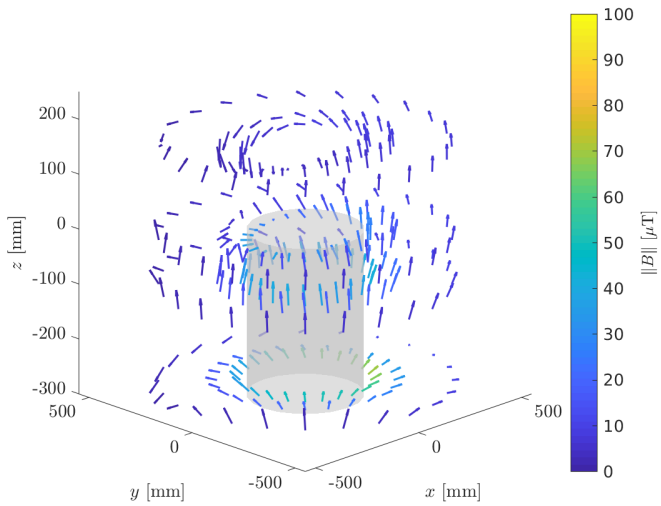

FIGURE 7: MAGNETIC STRAY FIELD AROUND THE HEAD OF THE CYLINDER WHEN MAGNETISED "UPWARDS" WITH 80 A/M.

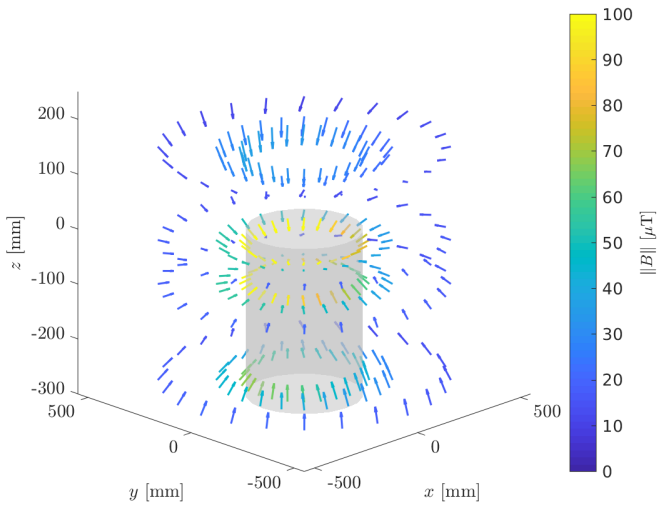

FIGURE 8: MAGNETIC STRAY FIELD AROUND THE HEAD OF THE CYLINDER AFTER BEING MAGNETISED "UPWARDS" WITH 80 A/M AND THEN LOADED WITH FIVE 1000 MM DROPS.

4.3. Convergence to magnetic equilibria

Figure 7 shows the magnetic field around the head of the pile after being magnetised "upwards" with 80 A/m. The background field, as shown in figure 6, was subtracted from the data, so figure 7 shows only the stray field due to the presence of the cylinder. The size of the vector is normalised for better visibility and the magnitude is indicated by different colours. Ring 10 – the closest to the installed coil – is clearly affected by the magnetisation of the pile as it points mostly outwards in radial direction with a magnitude up to 70 μT. The field is far less affected by the magnetised cylinder in other locations, as the flux rapidly falls to zero (dark blue vectors).

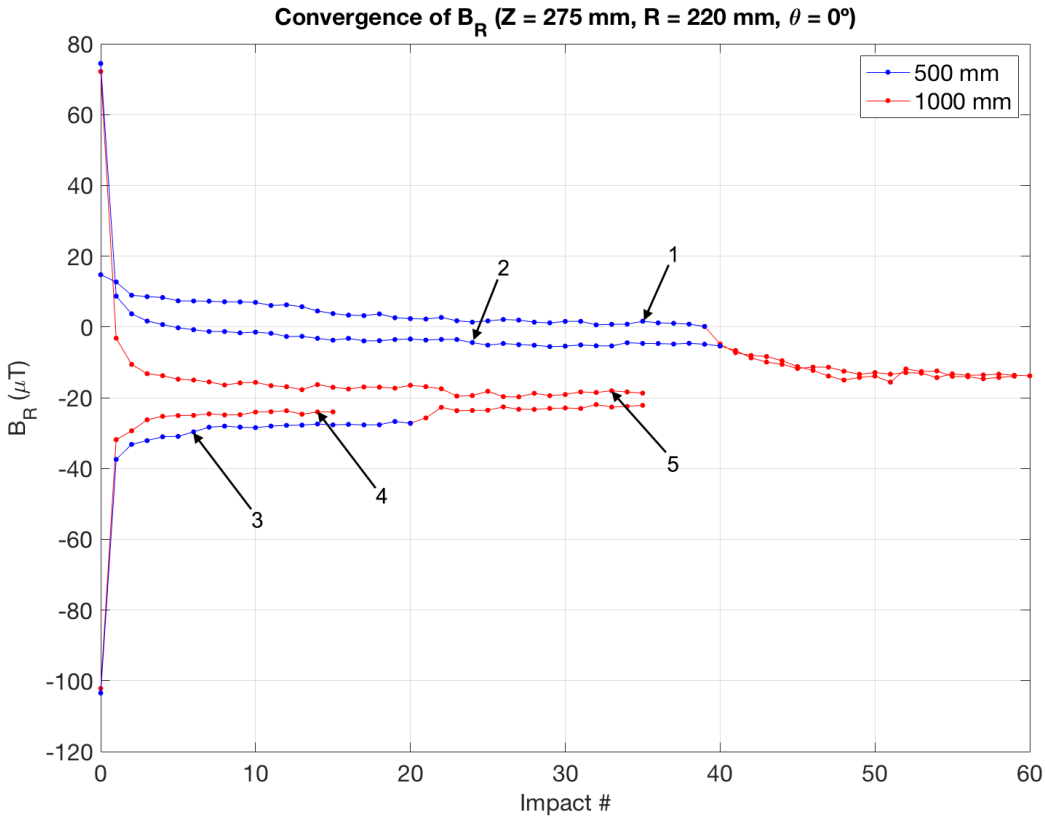

FIGURE 9: CONVERGENCE OF THE RADIAL MAGNETIC FLUX ON RING 10 AT θ = 0°.

Figure 8 shows the magnetic field after the cylinder was loaded with 5 impacts of 1000 ± 5 mm drops. The field clearly represents that of the south pole of a bar magnet, or a typical dipole, with a magnitude of up to 93 μT on ring 4. As the effect of magnetisation is the most visible in ring 10, the focus lies on this particular location from now on. Here, the change in the radial direction is the most affected by the impacts.

Figure 9 shows the change in magnetic flux in the radial direction on ring 10 at $\theta = 0º$ for tests one through five. Impacts from 500 mm are indicated in a blue colour, while impacts from 1000 mm are indicated in a red colour. A few observations are made:

- In all cases, a large irreversible change in magnetic flux can be seen after the first impact. Small irreversible changes can be seen after subsequent impacts, but in all cases the magnetic flux converges to an equilibrium state.
- Upon increasing the load from 500 mm to 1000 mm, a new irreversible change occurs that results in a new equilibrium state after a couple of impacts. Again, the first impact at a higher load shows the largest change. This result is in accordance with Atherton et al. (1984) and Li et al. (2017).
- Multiple equilibrium states that may or may not coincide are observed, seemingly independent of their original magnetic state and the impact load. Test 1 and 2 do reach the same magnetic state after the impact load is increased to 1000 mm. Test 3 and 4 reach the same magnetic state within the margin of error.

4.4. Induced plasticity

Figure 10 shows the change in radial flux of ring 10 for test 6. The cylinder was hit five times from 1000 mm, with – again – a dramatic change in magnetisation after the first hit. The cylinder was then consecutively hit five times from 1500 mm, eight times from 2000 mm and four times from 2500 mm. Starting from the second drop of 2500 mm (20th drop total), plastic deformation started to occur at the edge of the cylinder between$\theta = -90º$ and $\theta = 60º$, as shown in figure 11.

By increasing the drop height, the radial flux shows a steady increase towards the cylinder until it converges at 33.6 μT after 19 impacts total. After plastic deformation occurs (starting at the 20th impact), a decrease in radial flux is measured (indicated in red). The change in the magnetic field due to the plastification of the cylinder is particularly visible when looking at the angle of the field in the R-Z plane on ring 10, directly below the plastified edge.

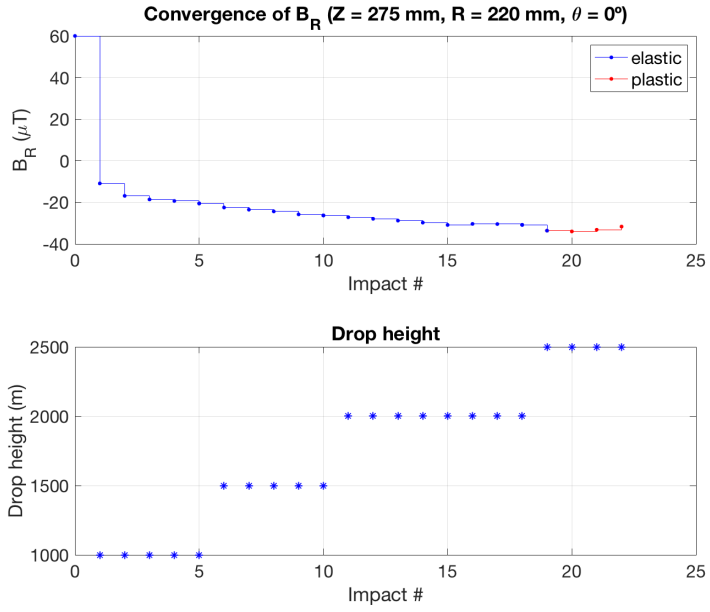

FIGURE 10: CONVERGENCE OF RADIAL FLUX WITH INCREASING DROP HEIGHT AND PLASTIC DEFORMATION.

FIGURE 11: PLASTIC DEFORMATION AT THE EDGE OF THE CYLINDER.

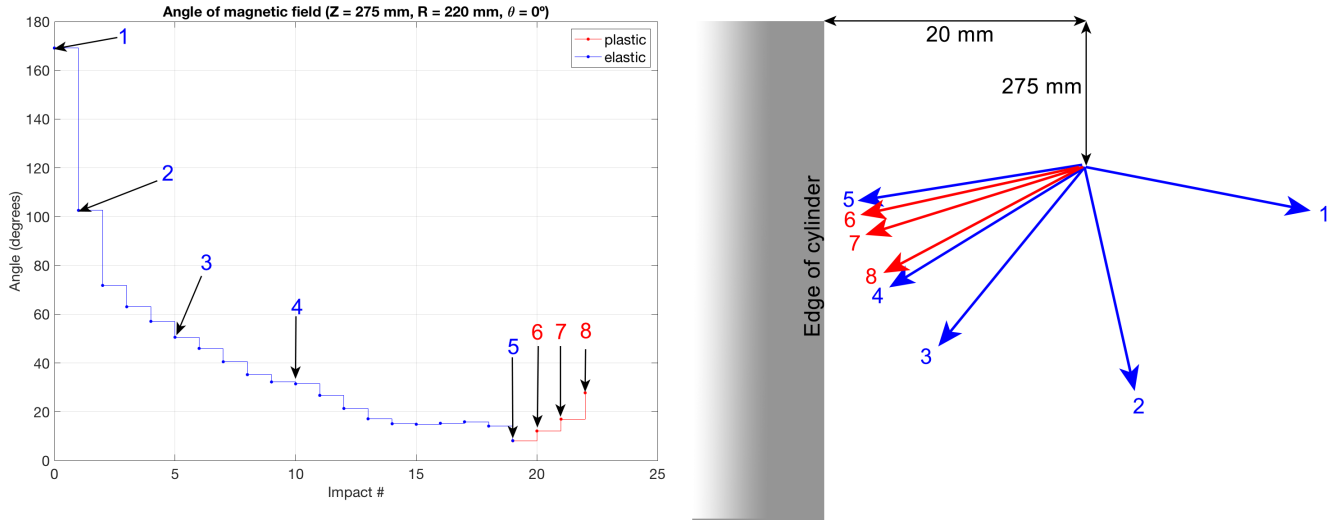

FIGURE 12: CHANGE IN ANGLE OF MAGNETIC FIELD VECTOR ON RING 10 AT θ = 0º. ANGLE VERSUS IMPACT (LEFT) AND GRAPHICAL REPRESENTATION OF THE ANGLE (RIGHT).

Figure 12 shows a vector plot (vector lengths are normalised for better visibility) that indicates the angle of the magnetic field on ring 10. Initially, the field points away from the cylinder under an angle of 169º. Upon hitting the cylinder multiple times, the angle converges towards the pile at an angle of 8º after 19 hits total. When plastic deformation starts to occur, the angle deviates from the trend and increases again in the opposite direction.

5. Discussion

5.1. Elastic regime

The magnetic field shows a large, irreversible change after the first impact caused by the drop weight and continually decreasing irreversible changes after consecutive impacts. This result is in accordance with findings of Atherton et al. (1984) and Li et al. (2017) for quasi-static loading cycles.

According to Atherton et al. (1984), “the magnetisation change over the first stress cycle is large and irreversible because the strain energy supplied exceeds some domain pinning energies and the domain walls move closer to ideal (anhysteretic) equilibrium.” Consecutive load cycles of the same magnitude produce smaller or no irreversible changes because further large-scale domain wall motions are not energetically favoured. This result is different from the quasi-static experiment by Li et al. (2017) who reported no irreversible change after the first load cycle. This difference could be explained due to the dynamic nature of loading, where the loading speed is much higher (Bao et al., 2017). When the previous peak stress is exceeded, the magnetic changes are large and irreversible again, like for the first load cycle, because the supplied strain energy exceeds the pinning energy again. This observation is in accordance with previous experiments by Li et al. (2017).

When looking at the order of initial magnetisation of tests 1 through 5, it appears that the final magnetic state stays close between subsequent tests. Although no tests from 500 mm reach the same equilibrium state when their initial magnetic states are different, the radial flux from tests 1 and 2 after repetitive 1000 mm impacts converge to the same level. Tests 3 and 4 have a very different initial magnetic state and do not converge to the same level as test 1 and 2, but do converge to a very similar level. For test 5, the initial radial flux is the same as for test 2 (and thus very different from test 4), but it converges to a level in between those of test 2 and 4.

A possible explanation for this behaviour is that the cylinder was not in the same initial magnetic state globally, despite the same flux reading on a local level, as shown in figure 9. This could be verified by repeating a similar experiment, while varying the order of initial magnetic states with and without fully demagnetising the sample in between tests.

However, Makar and Atherton (1995) showed that the magnetisation does not necessarily converge towards the global equilibrium state; they found that the magnetisation changes towards a local equilibrium

state. Xu et al. (2012) call this local equilibrium M_0; it represents a state where, in contrast to the anhysteretic state M_{an}, not all pinning sites have been overcome.

5.2. Plastic regime

When the sample starts to deform at the edge on the 20th impact, the change in magnetic flux is quite significant. It is not only measured on ring 4 that is closest to the deformed edge, but on rings 7 and 10 as well.

According to Sablik et al. (2004), plastic deformation affects the hysteretic magnetic properties of steel because it changes the dislocation density, which affects domain-wall movement and pinning, and also because it places the specimen under residual strain. Residual strains were found throughout the sample that, in combination with added pinning sites, can lead to the change in magnetic flux as shown in figure 10 and 12.

This change can also partially be explained by the permanent change in geometry of the sample. The coordinates of measurement points remain unchanged, which leads to the fact that the edge of the cylinder has come approximately 5 mm closer to measurement ring 4. However, it can be expected that the geometry change at the top will have much less influence on measurements taken on ring 10, where there are no visible changes to the geometry of the cylinder.

6. Conclusions

With this research, it can be concluded that the magnetisation of a steel cylinder with unknown initial magnetisation will reach a specific but not consistent equilibrium state from repeated impact loading within the elastic regime. It was observed that in all cases, a reversible and an irreversible change in measured magnetic flux occurred upon hitting the cylinder, where the irreversible change is the biggest on the first cycle. The irreversible changes in magnetisation converge to an equilibrium state, typically within 5 to 10 hits, after which no irreversible changes are observed without increasing the impact load. These equilibrium states do not necessarily coincide, unlike the model of Jiles (1995) predicted. Reversible changes upon impact, i.e. when stress changes, are still observed.

When the magnetisation has reached an equilibrium state, no irreversible change occurs with the same load. When the load is then increased, irreversible changes in the magnetisation are again observed, which will then quickly converge to a new equilibrium state. This suggests that the anhysteretic state cannot in all cases be reached, because energy barriers in the domain walls due to pinning sites need to be overcome. A local equilibrium state may therefore be energetically favourable. The fact that the measured magnetic flux of multiple (but not all) equilibrium states coincide, could suggest that discrete equilibrium states exist, which could be seen in the form of energy wells. It can be concluded that the equilibrium position that is reached, depends on the maximum induced stress level and the initial magnetic state. The magnetic and mechanical history of the specimen is therefore highly relevant.

When an equilibrium state is reached, it is possible to distinct irreversible changes in magnetisation from different causes and thus to detect plasticity. Given that the equilibrium states still change when the load is increased, it is important to load the cylinder as close as possible to the yield limit of the material, without exceeding it. When loading the cylinder with increasing stress within the elastic regime, the change in magnetisation and the equilibria that are achieved will follow a trend towards the anhysteretic state. When plastic deformation occurs, a deviation from this trend is observed. This deviation separates the irreversible change caused by plasticity from irreversible changes due to hysteresis.

In uncontrolled environments, it does not appear to be possible to predict the magnetic equilibrium state of the pile as the anhysteretic state is not reached. However, the equilibria that are found after repeated impacts in the elastic regime are still usable for practical applications of this technique, because of the trend deviation. As such, plastic deformation detection based on magnetic stray field analysis seems a viable option.

Acknowledgements

We would like to thank the technical staff at Stevinlab II and DEMO for their assistance and valuable ideas: Peter de Vries, Kees van Beek, Ruben Kunz, Fred Schilperoort, Giorgos Stamoulis, John Hermsen, Leon Roessen, Martin van der Meer, Ton Blom and Maiko van Leeuwen.

References

(1) Atherton, D., & Jiles, D. (1983). Effects of stress on the magnetization of steel. IEEE Transactions on Magnetics, 19(5), 2021–2023. https://doi.org/10.1109/TMAG.1983.1062784

(2) Atherton, D., Welbourn, C., Jiles, D., Reynolds, L., & Scott-Thomas, J. (1984). Stress-induced magnetization changes of steel pipes–Laboratory tests, Part II. IEEE Transactions on Magnetics, 20(6), 2129–2136. https://doi.org/10.1109/TMAG.1984.1063572

(3) Bao, S., & Gong, S. F. (2012). Magnetomechanical behavior for assessment of fatigue process in ferromagnetic steel. Journal of Applied Physics, 112(11), 113902. https://doi.org/10.1063/1.4769364

(4) Bao, Sheng, Gu, Y., Fu, M., Zhang, D., & Hu, S. (2017). Effect of loading speed on the stress-induced magnetic behavior of ferromagnetic steel. Journal of Magnetism and Magnetic Materials, 423(Supplement C), 191–196. https://doi.org/10.1016/j.jmmm.2016.09.092

(5) Craik, D. J., & Wood, M. J. (1970). Magnetization changes induced by stress in a constant applied field. Journal of Physics D: Applied Physics, 3(7), 1009. https://doi.org/10.1088/0022-3727/3/7/303

(6) Jiles, D. C. (1988). The effect of compressive plastic deformation on the magnetic properties of AISI 4130 steels with various microstructures. Journal of Physics D: Applied Physics, 21(7), 1196. https://doi.org/10.1088/0022-3727/21/7/023

(7) Jiles, D. C. (1995). Theory of the magnetomechanical effect. Journal of Physics D: Applied Physics, 28(8), 1537. https://doi.org/10.1088/0022-3727/28/8/001

(8) Jiles, D. C., & Atherton, D. L. (1984). Theory of the magnetisation process in ferromagnets and its application to the magnetomechanical effect. Journal of Physics D: Applied Physics, 17(6), 1265. https://doi.org/10.1088/0022-3727/17/6/023

(9) Li, Z., Dixon, S., Cawley, P., Jarvis, R., Nagy, P. B., & Cabeza, S. (2017). Experimental studies of the magneto-mechanical memory (MMM) technique using permanently installed magnetic sensor arrays. NDT & E International, 92(Supplement C), 136–148. https://doi.org/10.1016/j.ndteint.2017.07.019

(10) Makar, J. M., & Atherton, D. L. (1995). Effects of isofield uniaxial cyclic stress on the magnetization of 2% Mn pipeline steel - behavior on minor hysteresis loops and small major hysteresis loops. IEEE Transactions on Magnetics, 31(3), 2220–2227. https://doi.org/10.1109/20.376241

(11) Maylin, M. G., & Squire, P. T. (1993). Departures from the law of approach to the principal anhysteretic in a ferromagnet. Journal of Applied Physics, 73(6), 2948–2955. https://doi.org/10.1063/1.353026

(12) Meijers, P. C., Tsouvalas, A., & Metrikine, A. V. (2018). A non-collocated method to quantify plastic deformation caused by impact pile driving. International Journal of Mechanical Sciences, 148, 1–8. https://doi.org/10.1016/j.ijmecsci.2018.08.013

(13) Pitman, K. C. (1990). The influence of stress on ferromagnetic hysteresis. IEEE Transactions on Magnetics, 26(5), 1978–1980. https://doi.org/10.1109/20.104589

(14) Sablik, M. J., Geerts, W. J., Smith, K., Gregory, A., Moore, C., Palmer, D., … Campos, M. F. de. (2010). Modeling of Plastic Deformation Effects in Ferromagnetic Thin Films. IEEE Transactions on Magnetics, 46(2), 491–494. https://doi.org/10.1109/TMAG.2009.2033456

(15) Sablik, M. J., Yonamine, T., & Landgraf, F. J. G. (2004). Modeling plastic deformation effects in steel on hysteresis loops with the same maximum flux density. IEEE Transactions on Magnetics, 40(5), 3219–3226. https://doi.org/10.1109/TMAG.2004.832763

(16) Viana, A., Rouve, L.-L., Cauffet, G., & Coulomb, J.-L. (2010). Magneto-Mechanical Effects Under Low Fields and High Stresses - Application to a Ferromagnetic Cylinder Under Pressure in a Vertical Field. IEEE Transactions on Magnetics, 46(8), 2872–2875. https://doi.org/10.1109/TMAG.2010.2043825

(17) Viana, A., Coulomb, J.-L., Rouve, L.-L., & Cauffet, G. (2010). Numerical resolution of the modified Langevin equation using a differential expression: Application to the Jiles magnetostriction law of

approach. Journal of Magnetism and Magnetic Materials, 322(2), 186–189. https://doi.org/10.1016/j.jmmm.2009.07.068

(18) Xu, M., Xu, M., Li, J., & Xing, H. (2012). Using Modified J–A model in MMM detection at elastic stress stage. Nondestructive Testing and Evaluation, 27(2), 121–138. https://doi.org/10.1080/10589759.2011.622758

3 Additional findings

3.1. Dynamic measurements

In addition to measuring the static magnetic field in between blows, measurements were also recorded during the impact to see how the change in the magnetic field correlates to the induced stress wave. In order to do so, an Anisotropic Magnetic Resistance sensor — or AMR-sensor — is placed directly next to a strain gauge at a distance of approximately 25 mm from the pile. The strain measurements from the strain gauge and the magnetic flux measurements are recorded at a rate of 50 kHz.

Figure 3.1 shows a typical time-strain signal as it is recorded by the strain gauges at $z = 200$ mm together with the corresponding magnetic flux reading in the radial direction, during the first impact after magnetisation. The signal shows multiple peaks with decreasing magnitude over a period of approximately 1.5 s, because the drop weight bounces of the pile a few times. Upon the first hit, a significant irreversible change and some fluctuations are observed. Consecutive hits, as a result of the bouncing, are much smaller and do not show any irreversible changes.

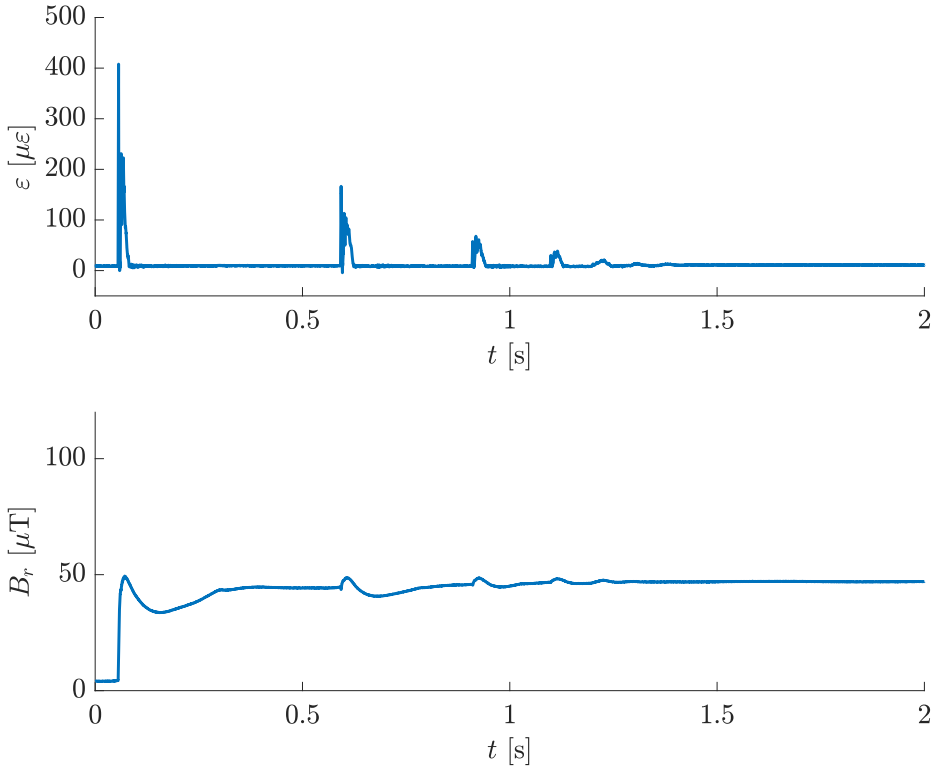

FIGURE 3.1: TIME-STRAIN SIGNAL AND MAGNETIC FLUX SIGNAL DURING FIRST BLOW AFTER MAGNETISATION.

In figure 3.2, the first impact is shown in more detail as a time-stress signal where it is assumed that:

$$\sigma = E\varepsilon. \tag{3.1}$$

The stress signal of each blow consists of multiple peaks, because the collision between the drop weight and the cylinder is not perfectly inelastic. Figure 3.2 clearly shows some reversible change in the magnetic measurement and a significant irreversible change. Changes in magnetisation occurs during and after stressing, while the latter should not occur. The reason for this is that the cylinder undergoes rigid body motions, while the AMR-sensor remains stationary. These low-frequency rigid body motions are also picked up by the sensor.

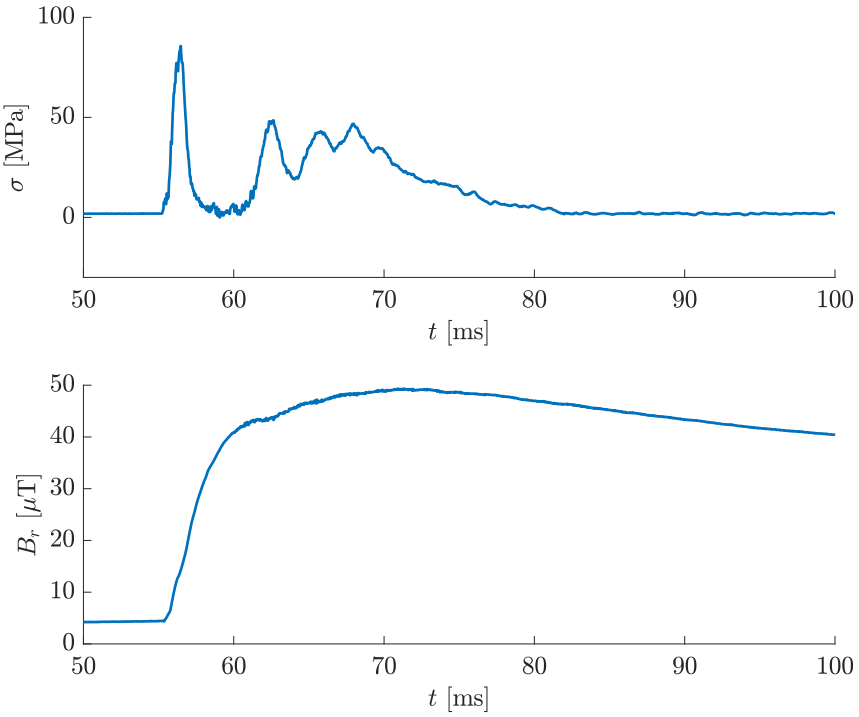

FIGURE 3.2: TIME-STRESS SIGNAL AND MAGNETIC FLUX SIGNAL DURING FIRST PEAK OF FIRST BLOW AFTER MAGNETISATION.

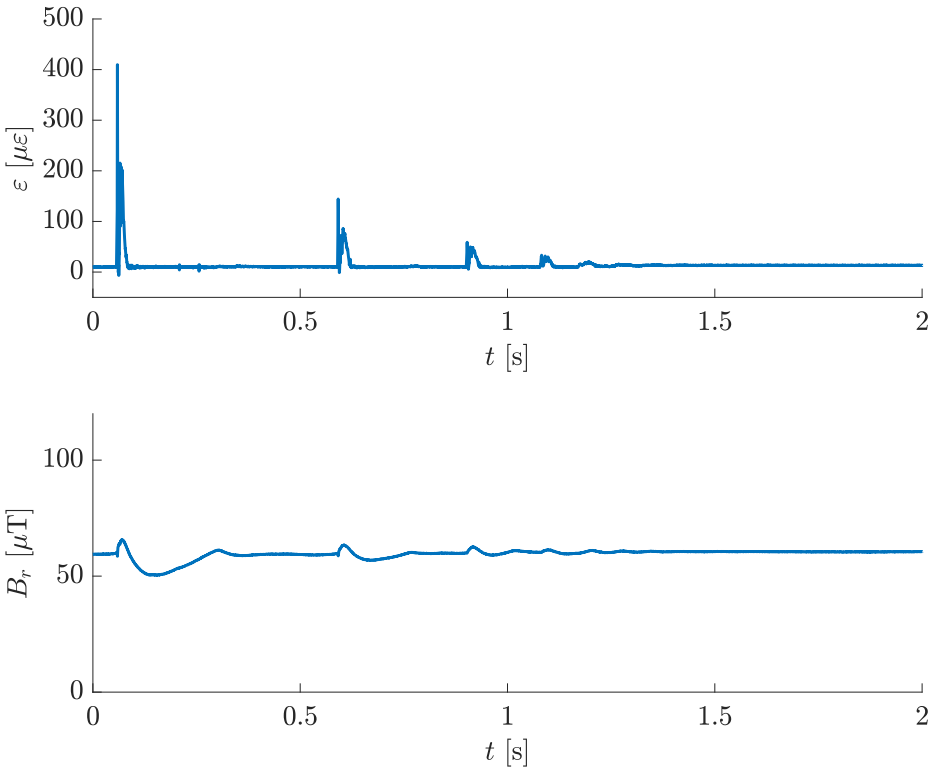

FIGURE 3.3: TIME-STRAIN SIGNAL AND MAGNETIC FLUX SIGNAL DURING SIXTH BLOW AFTER MAGNETISATION.

Figure 3.3 shows the full time-strain signal and radial magnetic flux signal of the sixth blow after magnetisation. In contrast to the first blow, as shown in figure 3.1, the measured magnetic flux does not show any irreversible change after loading. Figure 3.4 shows the signals during the first peak in more detail, analogue to figure 3.2.

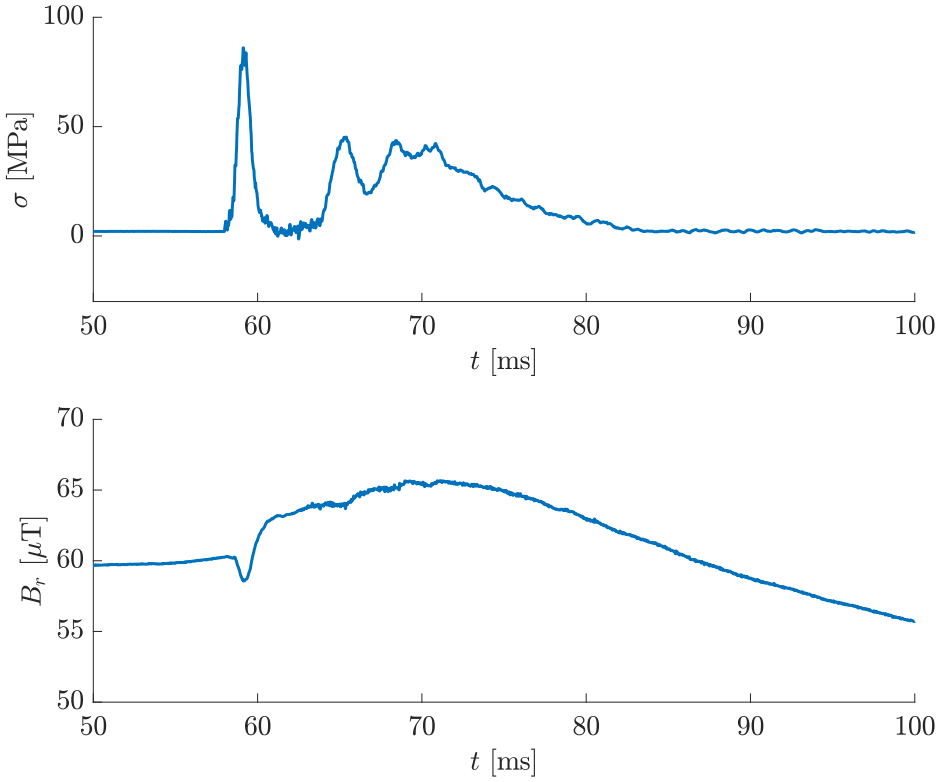

FIGURE 3.4: TIME-STRESS SIGNAL AND MAGNETIC FLUX SIGNAL DURING FIRST PEAK OF SIXTH BLOW AFTER MAGNETISATION.

Without the irreversible changes in magnetisation during stressing, the correlation between stress and magnetic flux has become clearer. However, the individual peaks in the stress signal are still not visible in the magnetic signal. Furthermore, there is also a noticeable low frequency component in the magnetic signal due to rigid body motions that is not directly visible in the stress signal.

In order to distill the flux changes due to the magnetomechanical effect, and thus find the relation with the stress signal, one should account for the rigid body motions. Given that these motions happen at a much lower frequency than the waves travel in the material, one could apply a high-pass filter on the frequency spectrum of both signals to cancel the effects of rigid body motion. These filtered signals are shown in figure 3.5.

In figure 3.5, the unfiltered stress signal is given by the blue line and the filtered signal by the red line. When magnitude of the magnetic flux signal is normalised to the stress signal, the correlation between the signals becomes apparent, as shown in figure 3.6.

Although the signals do not match perfectly and the AMR-sensor shows considerably more noise that the strain gauge, the AMR-sensor can certainly be considered as a contactless alternative to the strain gauge when properly calibrated. Parameters include the distance of the sensor to the object, the geometry of the object and the magnetic properties of the material, which will mainly depend on the chemical composition of the steel. It is also very important to compensate for rigid body motions, by means of a high-pass filter, accelerometers or otherwise.

With these dynamic signals, it is possible to see both the reversible and irreversible changes in the magnetic stray field, unlike with the static field measurements in between blows. By analysing how the

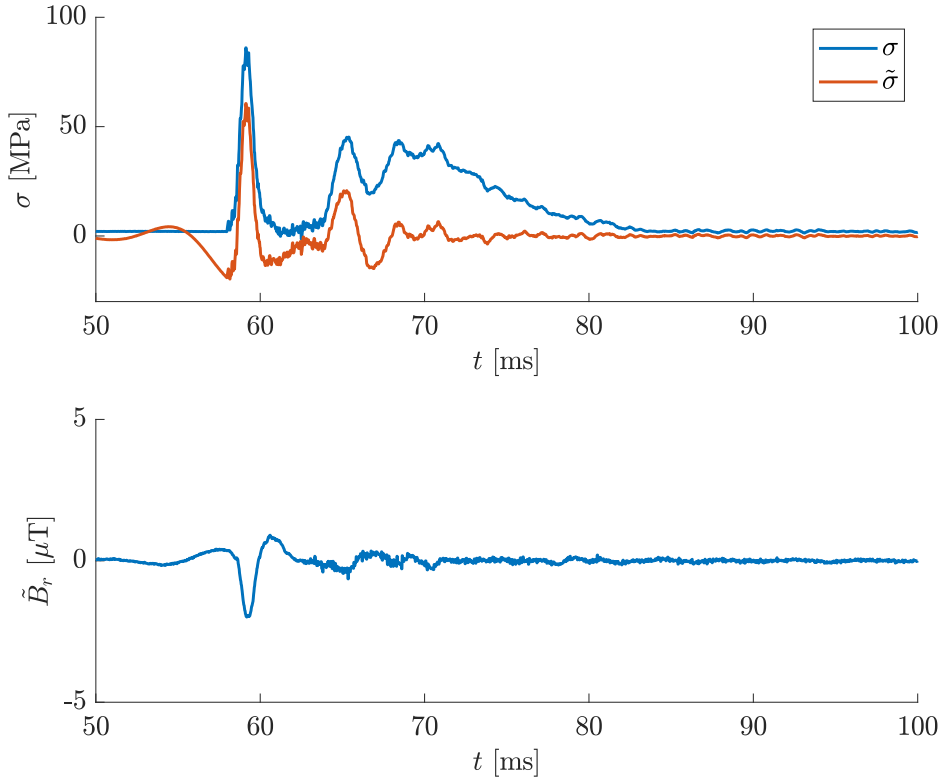

FIGURE 3.5: TIME-STRAIN SIGNAL AND MAGNETIC FLUX SIGNAL, FILTERED.

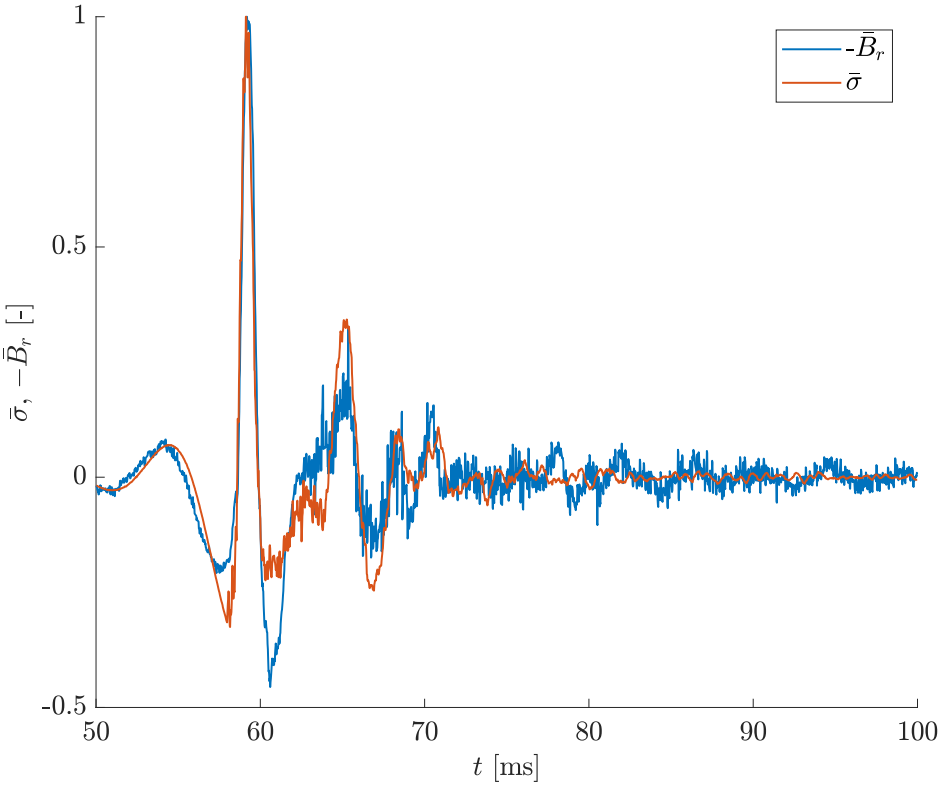

FIGURE 3.6: TIME-STRAIN SIGNAL AND MAGNETIC FLUX SIGNAL, FILTERED.

reversible changes evolve over the course of multiple impacts, it could potentially provide additional information on how domains change and what effects added pinning sites have on domain wall translation and domain wall bending.

Two cylinders were tested during the experiment, with different wall thicknesses. The first cylinder had a wall-thickness of 5 mm and the second cylinder had a wall thickness of 8 mm, of which the top 500 mm was machined down to 2.5 mm. The material composition of both samples is the same. Of both samples, extensive data is available. If this data is analysed and compared, it could provide some answers on how to calibrate the magnetic flux measurements for the geometry of the object, in particular the wall thickness.

3.2. Sensors

Multiple types of magnetic sensors were tested, of which the following can be concluded:

1. Search coils are the simplest type of magnetometers. It consists of a copper wire that is tightly wound as a coil. When the magnetic flux inside the coil changes, it induces a current in the coil which can be measured. Because it relies on a change in magnetic flux, it is not possible to measure static magnetic fields. Furthermore, it is difficult to measure very small changes in the magnetic field because the induced current in the coil is also very low. This type of magnetic sensors is unsuitable for our goal.

2. A Hall magnetometer or Hall effect sensor is a transducer that produces a voltage in response to a magnetic field, based on the Hall effect. Hall magnetometers cover a wide range of field strengths with a decent amount of precision. They are commonly used for proximity switches, positioning, speed detection and current sensing applications. These sensors are very small, very cheap and widely available.

   Hall magnetometers have an advantage over inductive sensors in that Hall magnetometers can detect static magnetic fields, while inductive sensors respond to a changing magnetic field to induce a current in a coil. Another benefit is that it is quite fast with bandwidths that go up into tens of kilohertz, which is necessary to measure the dynamic behaviour of the magnetic field on impact. The sensitivity varies either by the bias current or by changing the amplification of the voltage signal. Therefore, we can cover a large range of magnetic fields with a single sensor.

   While we were able to detect most irreversible and some reversible changes in the magnetic stray field during impacts, the signal-to-noise ratio proved to be quite poor. Heavy filtering of the signal is necessary to detect any correlation to the time-strain signal.

3. Fluxgate magnetometers are focused on low-field measurements like the Earth's field and its disturbances. During World War II, fluxgate magnetometers where developed to detect submarines and and where later used to confirm the theory of plate tectonics by using them to measure shifts in the magnetic patterns on the sea floor. Fluxgates are also used for navigation in maritime applications.

   The fluxgate magnetometer is very accurate and due to its focus on low-field measurements the preferred choice for this experiment. The fluxgate magnetometer that was used in this experiment, measures the flux of all three components of the magnetic field with a resolution of 1 nT. It is significantly larger than the other sensor types, but still compact enough for easy use. The downside of the fluxgate sensor is its relatively high price and its low operating frequency, which tops out at around 1 kHz. It has proven to be exceptionally useful for measuring static fields, but it is not fast enough to detect the reversible changes during impact.

4. Anisotropic Magnetoresistors (or AMR-sensors) are a type of magnetometers based on the magnetoresistive effect, which is the tendency of a material to change the value of its electrical resistance in an externally applied magnetic field.

   Magnetoresistive sensors are well suited for medium field strengths like the earth's field and are commonly used for field navigation and positioning measuring systems and read-heads for data storage devices. They can be manufactured at small sizes and low cost, which makes them attractive for mass-market consumption.

   AMR-sensors share some of the advantages of Hall-effect sensors. They can be relatively small and and can be produced at low cost. Like Hall-effect sensors and fluxgate magnetometers, they can detect static

fields. The most significant benefit for our application is that it is also very fast and can easily measure at 50 kHz or more, which is necessary to measure the dynamic behaviour of the magnetic field on impact. The signal-to-noise ratio is significantly higher compared to Hall-effect sensors, which makes it the best choice for our application.

The downside of AMR-sensors compared to Hall-effect sensors is that, as it is made from a ferromagnetic material, it suffers from magnetic hysteresis. This effect can offset the reading, as the sensor can be magnetised without an external magnetic field present. To remedy this problem, it needs to be demagnetised regularly.

4 Conclusion & recommendations

4.1. Conclusion

With this research, it can be concluded that the magnetisation of a steel cylinder with unknown initial magnetisation will reach a specific but not consistent equilibrium state from repeated impact loading within the elastic regime. It was observed that in all cases, a reversible and an irreversible change in measured magnetic flux occurred upon hitting the cylinder, where the irreversible change is the biggest on the first cycle. The irreversible changes in magnetisation converge to an equilibrium state, typically within 5 to 10 hits, after which no irreversible changes are observed without increasing the impact load. These equilibrium states do not necessarily coincide, unlike the model of Jiles (1995) predicted. Reversible changes upon impact, i.e. when stress changes, are still observed.

When the magnetisation has reached an equilibrium state, no irreversible change occurs with the same load. When the load is then increased, irreversible changes in the magnetisation are again observed, which will then quickly converge to a new equilibrium state. This suggests that the anhysteretic state cannot in all cases be reached, because energy barriers in the domain walls due to pinning sites need to be overcome. A local equilibrium state may therefore be energetically favourable. The fact that the measured magnetic flux of multiple (but not all) equilibrium states coincide, could suggest that discrete equilibrium states exist, which could be seen in the form of energy wells. It can be concluded that the equilibrium position that is reached, depends on the maximum induced stress level and the initial magnetic state. The magnetic and mechanical history of the specimen is therefore highly relevant.

When an equilibrium state is reached, it is possible to distinct irreversible changes in magnetisation from different causes and thus to detect plasticity. Given that the equilibrium states still change when the load is increased, it is important to load the cylinder as close as possible to the yield limit of the material, without exceeding it. When loading the cylinder with increasing stress within the elastic regime, the change in magnetisation and the equilibria that are achieved will follow a trend towards the anhysteretic state. When plastic deformation occurs, a deviation from this trend is observed. This deviation separates the irreversible change caused by plasticity from irreversible changes due to hysteresis.

In uncontrolled environments, it does not appear to be possible to predict the magnetic equilibrium state of the pile as the anhysteretic state is not reached. However, the equilibria that are found after repeated impacts in the elastic regime are still usable for practical applications of this technique, because of the trend deviation. As such, plastic deformation detection based on magnetic stray field analysis seems a viable option.

When the dynamic magnetic measurements are compared to the time-strain signal from the installed strain gauges, a clear correlation can be seen when a high-pass filter is applied in order to account for rigid body motions. Although the signals do not match perfectly and the AMR-sensor shows considerably more noise that the strain gauge, the AMR-sensor can certainly be considered as a contactless alternative to the strain gauge when properly calibrated.

4.2. Recommendations

In order to make this new technique for strain- and plasticity detection a viable option in practise, further research is necessary to improve the knowledge on this subject. For further research, a few recommendations can be made.

4.2.1. Improving the set-up

Although the experimental set-up was carefully designed and has provided valuable data, some improvements can be made.

We set out to do the experiment on a large scale object, in order to resemble a real monopile as close as possible. While this was certainly an important aspect of the research, it also made the experiment quite difficult to execute due to the large size and weight of the components, despite the availability of a crane.

Installation of and repairs to the set-up were very time consuming and assistance from technical staff was often necessary. At times it was also difficult to get accurate measurements due to large tolerances in numerous variables, although these issues will also occur during actual pile driving processes. Scaling down and simplifying the set-up would likely improve the accuracy of measurements and make it easier to execute the experiment.

In order to magnetise the cylinder, we tightly wound a copper wire around it to which a current can be applied. This coil was concentrated 500 mm from the top, as to generate a high magnetic field near that location. As a result, the magnetic field seamed only affected near the coil and much less around the top of the pile. This limits the usefulness of some of the measurements. Instead, it would probably have been better to distribute the windings over the entire pile, in order to achieve a more homogenous magnetisation.

In order to demagnetise the pile, we used a small coil connected to an AC power supply. The alternating current creates an alternating magnetic field in the coil. By swiping the coil past the cylinder, a decreasing amplitude in the applied magnetic field is mimicked which leads to demagnetisation of the pile. This technique works reasonably well, but the swiping needs to be done carefully and in a consistent manner. Limited mobility and obstructions due to wiring and other elements of the set-up makes it very difficult to demagnetise the pile evenly this way. Using an alternating current with a decreasing amplitude on an evenly distributed coil around the entire cylinder would have probably done a better job at evenly demagnetising the entire cylinder.

Using a drop weight to simulate a hydraulic impact hammer turned out to have a considerable draw back: due to small asymmetries on the impact surface and tilting of the weight, the recorded strain levels had significant deviations from the mean when the block was rotated a bit. Preventing the weight from rotating during lifting and falling is not always possible. With a hydraulic impact hammer, the induced stresses can be repeated much more consistently.

The lower boundary condition could be much simpler and better. Despite our best efforts to limit rigid body motions, the system of timber beams, a stainless steel plate and sand was insufficient to do so. The system was also very prone to damage and was difficult to repair. Instead, bolting the cylinder onto a heavy, solid block of concrete would probably have done a much better job.

4.2.2. Future testing

In this research, we have seen the anhysteretic state is typically not reached, but local equilibria are always reached that follow a trend towards the anhysteretic state with increased maximum stress. These equilibria appear to be sufficiently useable in order to detect plastic deformation, because we observed a deviation from this trend.

It should be further examined if this deviation always occurs, independent of the initial state and the equilibrium state that is reached before plastification. It should also be examined at which measurement locations the plastification can be detected and what enables or prohibits the detection.

More destructive testing needs to be done where initial magnetic states and resulting equilibria states are varied. This test can probably be done on a much smaller scale.

Another way to detect plastic deformation through magnetic stray field analysis should be investigated. Instead of monitoring the reminiscent magnetisation of the object, i.e. when no more external field is applied, one could monitor if the saturated magnetisation under a constant applied external field changes. In this test, a coil around the cylinder constantly applies a strong magnetic field around the pile, which should bring the magnetisation of the steel into saturation. This is the maximum field strength one would measure. If no plastic deformation occurs, the saturated magnetisation would likely not change. When plastic deformation occurs, the maximum magnetisation that can be induced would likely decrease.

4.2.3. Modeling

We have seen that the magnetic flux signal correlates very closely to the strain signal once the signal is normalised and filtered to account for rigid body motions. If you would want to model the strain signal based on the magnetic flux signal, this normalisation depends on a few parameters that need to be calibrated. These parameters include the geometry of the pile like diameter and wall thickness, the distance of the sensor to the pile, chemical composition of the pile and so on. Multiple tests need to be done to empirically calibrate these variables. Tests with varying wall thicknesses have already been done with data available.

Bibliography

(1) Atherton, D., & Jiles, D. (1983). Effects of stress on the magnetization of steel. IEEE Transactions on Magnetics, 19(5), 2021–2023. https://doi.org/10.1109/TMAG.1983.1062784

(2) Atherton, D., Welbourn, C., Jiles, D., Reynolds, L., & Scott-Thomas, J. (1984). Stress-induced magnetization changes of steel pipes–Laboratory tests, Part II. IEEE Transactions on Magnetics, 20(6), 2129–2136. https://doi.org/10.1109/TMAG.1984.1063572

(3) Bao, S., & Gong, S. F. (2012). Magnetomechanical behavior for assessment of fatigue process in ferromagnetic steel. Journal of Applied Physics, 112(11), 113902. https://doi.org/10.1063/1.4769364

(4) Bao, Sheng, Gu, Y., Fu, M., Zhang, D., & Hu, S. (2017). Effect of loading speed on the stress-induced magnetic behavior of ferromagnetic steel. Journal of Magnetism and Magnetic Materials, 423(Supplement C), 191–196. https://doi.org/10.1016/j.jmmm.2016.09.092

(5) Craik, D. J., & Wood, M. J. (1970). Magnetization changes induced by stress in a constant applied field. Journal of Physics D: Applied Physics, 3(7), 1009. https://doi.org/10.1088/0022-3727/3/7/303

(6) Griffiths, D. J. (2008). Introduction to Electrodynamics (3rd ed.). San Francisco, USA: Prentice Hall.

(7) Jiles, D. C. (1988). The effect of compressive plastic deformation on the magnetic properties of AISI 4130 steels with various microstructures. Journal of Physics D: Applied Physics, 21(7), 1196. https://doi.org/10.1088/0022-3727/21/7/023

(8) Jiles, D. C. (1995). Theory of the magnetomechanical effect. Journal of Physics D: Applied Physics, 28(8), 1537. https://doi.org/10.1088/0022-3727/28/8/001

(9) Jiles, D. C. (1998). Introduction to Magnetism and Magnetic Materials (2nd ed.). Boca Raton, USA: Taylor & Francis.

(10) Jiles, D. C., & Atherton, D. L. (1984). Theory of the magnetisation process in ferromagnets and its application to the magnetomechanical effect. Journal of Physics D: Applied Physics, 17(6), 1265. https://doi.org/10.1088/0022-3727/17/6/023

(11) Li, Z., Dixon, S., Cawley, P., Jarvis, R., Nagy, P. B., & Cabeza, S. (2017). Experimental studies of the magneto-mechanical memory (MMM) technique using permanently installed magnetic sensor arrays. NDT & E International, 92(Supplement C), 136–148. https://doi.org/10.1016/j.ndteint.2017.07.019

(12) Makar, J. M., & Atherton, D. L. (1995). Effects of isofield uniaxial cyclic stress on the magnetization of 2% Mn pipeline steel - behavior on minor hysteresis loops and small major hysteresis loops. IEEE Transactions on Magnetics, 31(3), 2220–2227. https://doi.org/10.1109/20.376241

(13) Maylin, M. G., & Squire, P. T. (1993). Departures from the law of approach to the principal anhysteretic in a ferromagnet. Journal of Applied Physics, 73(6), 2948–2955. https://doi.org/10.1063/1.353026

(14) Meijers, P. C., Tsouvalas, A., & Metrikine, A. V. (2018). A non-collocated method to quantify plastic deformation caused by impact pile driving. International Journal of Mechanical Sciences, 148, 1–8. https://doi.org/10.1016/j.ijmecsci.2018.08.013

(15) Pitman, K. C. (1990). The influence of stress on ferromagnetic hysteresis. IEEE Transactions on Magnetics, 26(5), 1978–1980. https://doi.org/10.1109/20.104589

(16) Ripka, P. (2001). Magnetic sensors and magnetometers. Boston, USA: Artech House.

(17) Sablik, M. J., Geerts, W. J., Smith, K., Gregory, A., Moore, C., Palmer, D., … Campos, M. F. de. (2010). Modeling of Plastic Deformation Effects in Ferromagnetic Thin Films. IEEE Transactions on Magnetics, 46(2), 491–494. https://doi.org/10.1109/TMAG.2009.2033456

(18) Sablik, M. J., Yonamine, T., & Landgraf, F. J. G. (2004). Modeling plastic deformation effects in steel on hysteresis loops with the same maximum flux density. IEEE Transactions on Magnetics, 40(5), 3219–3226. https://doi.org/10.1109/TMAG.2004.832763

(19) Tsouvalas, A. (2015). Underwater noise generated by offshore pile driving. https://doi.org/10.4233/uuid:55776f60-bbf4-443c-acb6-be1005559a98

(20) Viana, A., Rouve, L.-L., Cauffet, G., & Coulomb, J.-L. (2010). Magneto-Mechanical Effects Under Low Fields and High Stresses - Application to a Ferromagnetic Cylinder Under Pressure in a Vertical Field. IEEE Transactions on Magnetics, 46(8), 2872–2875. https://doi.org/10.1109/TMAG.2010.2043825

(21) Viana, A., Coulomb, J.-L., Rouve, L.-L., & Cauffet, G. (2010). Numerical resolution of the modified Langevin equation using a differential expression: Application to the Jiles magnetostriction law of approach. Journal of Magnetism and Magnetic Materials, 322(2), 186–189. https://doi.org/10.1016/j.jmmm.2009.07.068

(22) Xu, M., Xu, M., Li, J., & Xing, H. (2012). Using Modified J–A model in MMM detection at elastic stress stage. Nondestructive Testing and Evaluation, 27(2), 121–138. https://doi.org/10.1080/10589759.2011.622758

Appendix A Set-up images

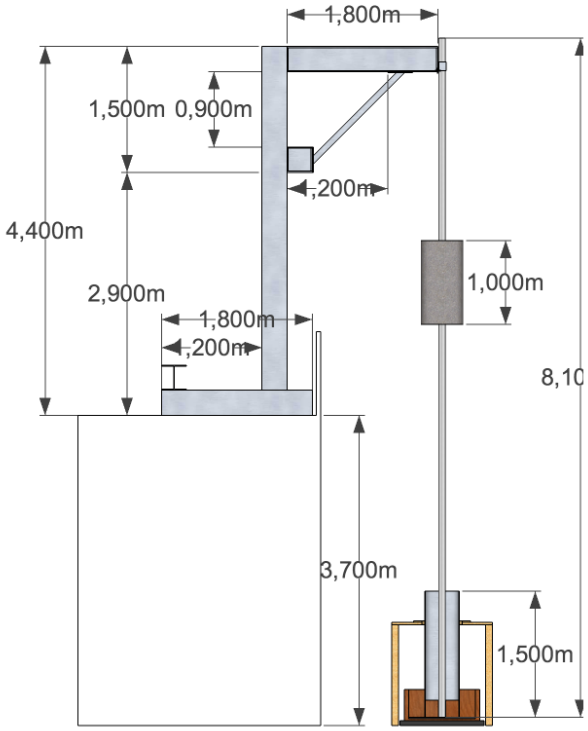

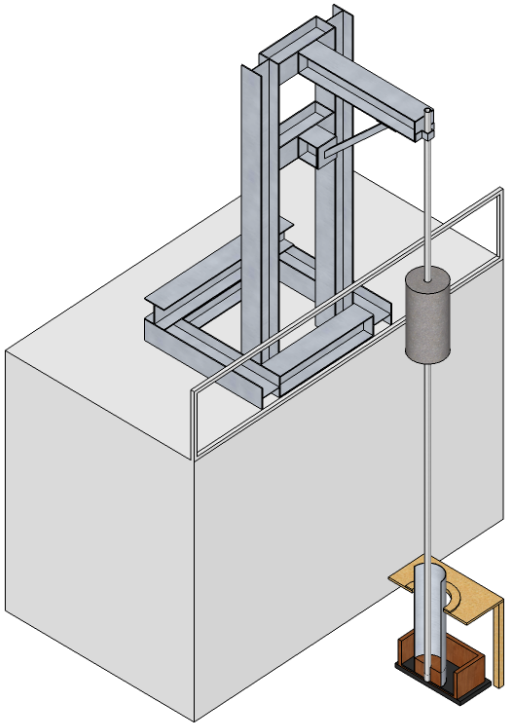

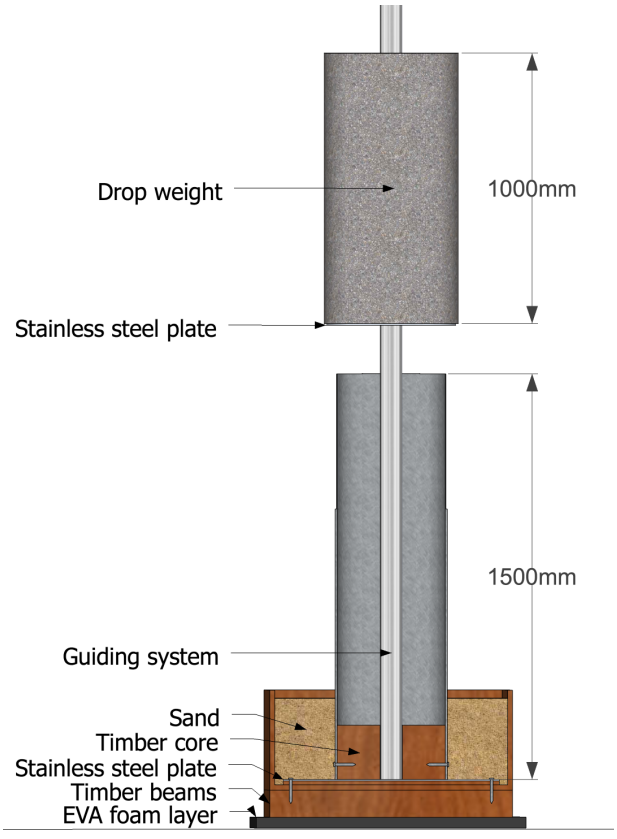

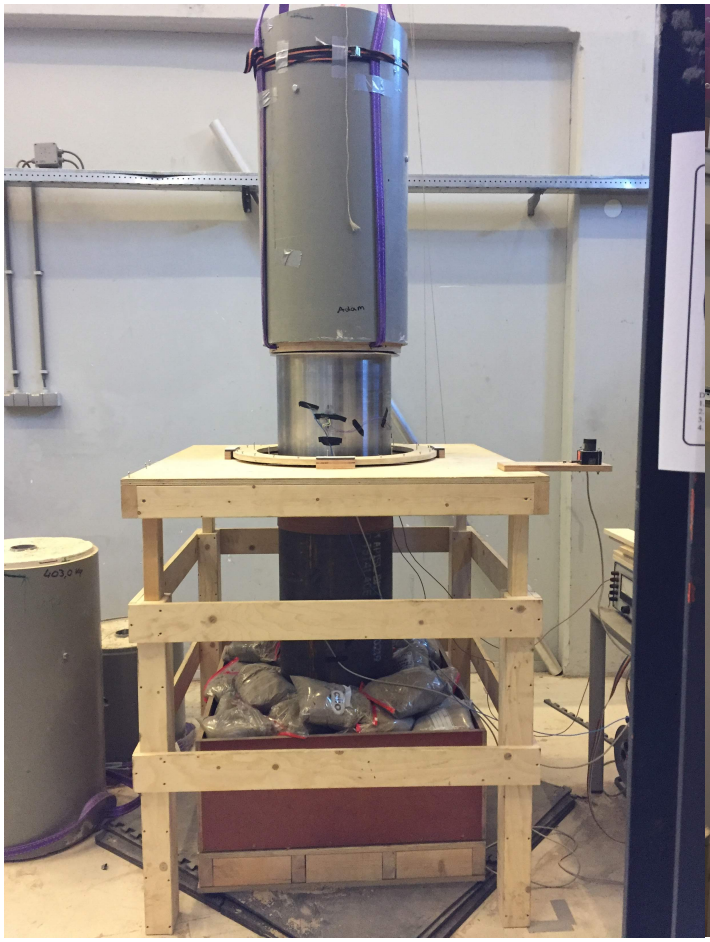
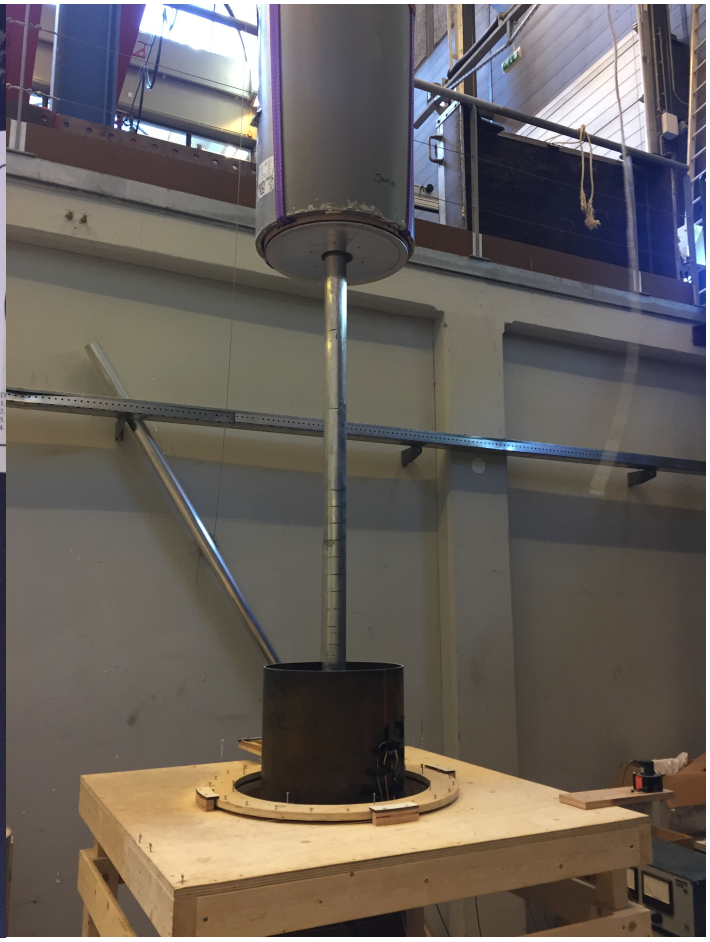

Adam
25
25